Erasmus Mundus Programme
M.Sc. programme in
Coastal and Marine Management

CoMEM

Tidal energy resources assessment in Indonesia

a case study in Alas Strait

Nicky Satyadharma Aziz

July 2009

Thesis work done at the University of Southampton

UNIVERSITY OF Southampton
School of Civil Engineering and the Environment

The Erasmus Mundus Master in Coastal and Marine Engineering and Management (CoMEM) is a two-year, English taught international Master's programme, in which five high-rated European universities participate. Focus is on the key issues involved in providing sustainable, environmentally friendly, legally and economically acceptable solutions to various problems in the CoMEM field.

The CoMEM MSc course is taught at five European universities:

* NTNU, Trondheim, Norway
* Delft Technical University, Delft, The Netherlands
* UPC, Barcelona, Spain
* City University, London, United Kingdom
* University of Southampton, Southampton, United Kingdom

The first year comprises two semesters of 30 ECTS each (course and project work), which will be spent at NTNU,Trondheim and Delft University respectively. This year provides academic and social coherence through a choice of compulsory and optional courses. It will establish a broad common foundation and prepare for the final year.

For the first half of the second year (one semester of 30 ECTS course and project work), three main routes with a particular emphasis are offered: either in environmental engineering at UPC, Barcelona, Spain, in environment and management at City University, London, or in business and management at the University of Southampton, Southampton, both in the United Kingdom. The third semester allows for specialisation in one of these three subjects. In the fourth and final semester a master's thesis at one of the three universities has to be made. The CoMEM programme therefore offers the following posibilities as illustrated in the diagram below:

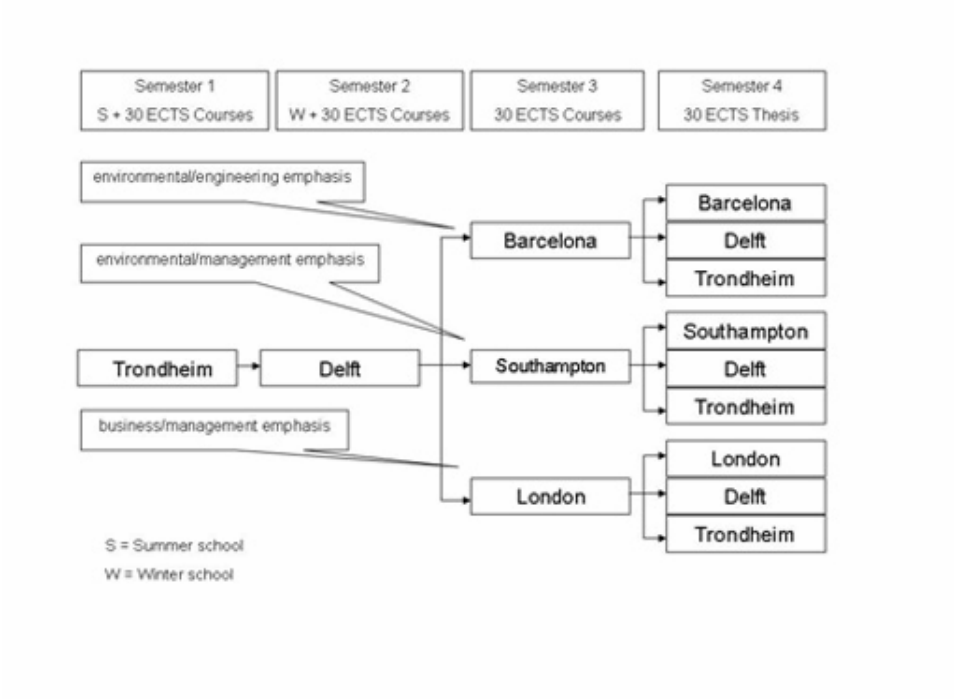

Information regarding the CoMEM programme can be obtained from the programme director'
prof.dr. Marcel J.F. Stive
Delft University of Technolgoy
Faculty of Civil Engineering and Geosciencese
PO Box 5048
2600 GA Delft
The Netherlands
comem@tudelft.nl

UNIVERSITY OF SOUTHAMPTON

FACULTY OF ENGINEERING, SCIENCE AND MATHEMATICS

SCHOOL OF CIVIL ENGINEERING AND THE ENVIRONMENT

TIDAL ENERGY RESOURCES ASSESSMENT IN INDONESIA

A CASE STUDY IN ALAS STRAIT

Nicky Satyadharma Aziz

A dissertation submitted in partial fulfilment of the degree of

Msc in Coastal and Marine Engineering and Management

July 2009

SUMMARY

With the instability of oil prices and the increasing of people's awareness in environmental problems, renewable energy is the key solution of these problems. Tidal energy, with its advantages of being predictable and its high energy density, is one of the most promising renewable energy forms. Indonesia's topographic conditions with plenty of narrow strait between the islands and its strategic location between two oceans make the tidal energy development in Indonesia looks promising.

This study is intended to assess tidal energy resources in Indonesia. A case study in Alas Strait, a pioneer study for this site, is selected among many prospective sites considering its relative shallow depth, high current velocity, and location which far from major shipping line. Princeton Ocean Model (POM) is used to model the flow pattern in the site. It uses the bathymetric map to represent the depth and applies tidal elevation in open boundary condition as generating force. The result from POM is then used to quantify the extractable energy resources using farm method.

The model result shows that current velocity in Alas Strait is relatively high, i.e. could reach up to 2 m/s in certain locations during spring tide. Array of typical Marine Current Turbine (MCT) is then placed in specific locations in Alas Strait (depends on water depth) to simulate the tidal energy extraction. New method of estimating downstream current velocity based on direction of the flow is applied to calculate the total power from the array. This results in 27.065 GWh/month for current MCT scenario with depth limitation and 52.736 GWh/month for floating MCT scenario.

To conclude, Alas Strait has the potential to be the location of MCT installation. This may be not feasible in the current time since the cost for implementing MCT is still relatively high. However, with the maturity of the technology, lower cost, and the urge to "go green", this will be applicable in the future.

ACKNOWLEDGEMENTS

Many people contribute in preparing this dissertation. Some help with the actual works on the thesis while others support and cheer me up when needed. This past two years has been a long journey, full of ups and down. Without their contribution, I would not be able to complete this dissertation.

Therefore I would like to express my gratitude to:

- Prof. A.S. Bahaj, my supervisor at the University of Southampton
- Luke Blunden for daily supervision on the project.
- Prof. Marcel Stive, Helena, Mariette, and Madelon.
- Prof. Nichols, Southampton CoMEM Coordinator
- All my professors and lecturers in Southampton, Delft, and Trondheim
- W. Pangastuti, A.M. Firdaus, and A. Wurjanto for all their help.
- My parents and family for all their prayer and support
- R. Ranasinghe and M. Hemer for helping me with POM
- All my CoMEM colleagues: Egon, Rahma, J.C, Abiy, Boss, Saravanan, Sid, Meghan, Stella, Rodrigo, Pavel, Katja, Maggie, Chris, and Thang
- All my friends in Southampton, Delft, and Trondheim.
- And last but not least my future wife, Maryani who is always be there for me.

TABLE OF CONTENTS

LIST OF FIGURES

LIST OF TABLES

GLOSSARY OF TERMS

Tidal Energy	Form of hydropower that converts the energy of tides into electricity or other useful forms of power
Tidal Devices	Devices that capture tidal energy to be convert to another form of energy
Alas Strait	Strait which separate Lombok Island with Sumbawa Island. It is located in Indonesian archipelago
Java Sea	Shallow sea on the Sunda Shelf located in between Java, Sumatra, Kalimantan, and Sulawesi

LIST OF ABBREVIATIONS

POM	Princeton Ocean Model
OBC	Open Boundary Condition
MCT	Marine Current Turbines
CFD	Computational Fluid Dynamics
ADCP	Acoustic Doppler Current Profiler
CFL	Courant-Friedrich-Lewy. CFL condition is a condition for convergence while solving partial differential equations numerically. It resulting in time step must be less than a certain time, otherwise the simulation will produce incorrect results.
ITS	Inverse Tidal Solution
SIF	Significant Impact Factor

1 INTRODUCTION

1.1 Problem Background

It is well known that conventional energy resources such as oil and gas could reach their limitation soon. Efforts that can be taken to reduce the burden from oil and gas include:

- Reduce energy use
- Create or invent more efficient technology (e.g. Hybrid in car)
- Renewable energy

From all the above possible solutions, renewable energy is the most compelling one since it is abundant yet often overlooked. This reason as well as the increase of people's awareness in environmental issues (e.g. global warming and sea level rise) caused by carbon burning (Intergovernmental Panel on Climate Change, 2007), promote the use and development of renewable energy.

One of the latest developments in renewable energy sector is the application of tidal power to generate energy. Tidal energy has advantages in its predictability compared to other marine renewable energy. Power generated by tidal current can be forecasted accurately since the change of the force that influences tidal current, i.e. distance of a certain location on earth's surface relative to the moon and the sun, is known beforehand. Another advantage is the similarity in energy extraction technology with a well established wind energy.

Indonesia, a developing country located in South East Asia, has the fourth biggest population in the world (Central Intelligence Agency, 2008). Having considerably high population, unfortunately, there are problems related to the share of energy in the country. These problems are even worsened by the recent increase of oil price, which force almost all provinces in Indonesia to experience a regulated electricity blackout. In fact, the electricity blackout does not solely happen in some underdeveloped provinces, but also occurs in the capital city, Jakarta. The major cause of these problems is due to the fact that most of electric power plants in Indonesia use oil as their source of energy (Indonesia's Centre for Data and Information on Energy and Mineral Resources , 2008a).

For the last five years, there is a significant yearly increase in Indonesia's energy consumption. On the other hand, the production of conventional energy experiences a

downturn (Indonesia's Centre for Data and Information on Energy and Mineral Resources, 2008b). This situation has forced Indonesia to become energy importer country, which never happened throughout its history.

In their paper, Hermawan and Hadi (2006) show that Indonesia has a lot of potentials in renewable energy. However, the share of this energy to the total energy mix is very low. Efforts should be taken to enhance the use of renewable energy, such as investment in research and development and creating renewable energy pilot project.

Currently, the development of renewable energy in Indonesia is regulated by Indonesia's Presidential Decree No.5 / 2006 regarding the national energy policy (Indonesia's Centre for Data and Information on Energy and Mineral Resources, 2006). This decree states that contribution of renewable energy in the 2025 is expected to be at 17% of the total national primary energy mix, of which 5 % should come from hydro power. The Hydro power mentioned is not limited to the conventional river generated electricity, but also includes marine renewable energy in the form of wave and tidal energy.

As the biggest archipelagic country worldwide, Indonesia has a great potential in implementing tidal energy sites considering its narrow channels and straits between the islands. Although the tidal range is much lower compared to some other places in the world (most notably is United Kingdom), the shape and bathymetry of some locations in Indonesia are expected to generate high current speeds which is suitable for tidal energy extraction.

However, even with the overwhelming facts above, research and efforts for the implementation of tidal energy in Indonesia is still considerably rare and unimpressive. In fact, most of the researches related to marine renewable energy in Indonesia had been focused solely on wave energy. Researches on tidal energy have been carried out just recently; one example is tidal energy assessment conducted by Pangastuti (2005). Tidal energy assessments in other prospective areas are needed to promote the implementation of tidal energy in Indonesia.

Tidal energy resources assessment is important for determining the total amount of energy (in electricity terms) that can be generated by tidal energy in the whole Indonesia. This also can be used in planning the implementation stage of the tidal

energy; site with higher potential in terms of electricity generation should be prioritised first. Other than that, selecting the first sites for tidal energy pilot project location is important to determine its suitability for future step.

Based on the above discussion, it is known that that an investigation of prospective sites for implementing tidal energy extraction In Indonesia is required. This study analyses the potential of operating a tidal energy site extraction. The assessment of electricity generation's pattern that would be expected from the development of tidal current electric generating systems is also included.

1.2 Aims and Objectives

This dissertation was initially aimed to determine the amount of energy that can be generated by tidal stream in Indonesia. However, due to several limitation to conduct a regional research scale (e.g. availability of the data and its accuracy), the above objective needs to be adapted.

Conducting tidal energy resource assessment for the whole Indonesia is either unrealistic or not viable. With so many possible tidal energy sites all over Indonesia, and limited computer power and time (high resolution model resulting in high accuracy but needs higher computation power and vice versa for low resolution model), creating an accurate model with high resolution is more reliable and useful since it represents more of the actual condition.

Therefore, it is decided to model only a site that can be categorised as a pilot project with high probability of realisation. The site will be modelled using a hydrodynamic model, i.e. Princeton Ocean Model (POM), which able to perform simulation that has an accurate result for the research.

Specific objectives of this research consist of:

1. Choosing an ideal site for the tidal energy resource assessment to be conducted.
2. Conducting a review of the relevant literature, setup, calibrate, and validate a POM model to effectively simulate the actual site condition.
3. Running the model in adequate time frame to obtain the actual tidal current flow velocity in the chosen location.

4. Analysing and quantifying the tidal energy resources in terms of electricity generation in a period of times.
5. Undertaking discussions of findings in context of comparable study in different places and evaluating the significance of the results with the limitation of the study.

It is expected by achieving the above objectives; the results may act as a stimulus for further research and will contribute towards the development of tidal energy in Indonesia. In addition, it is also expected that, in broader terms, this will contribute in solving energy problem in Indonesia.

1.3 Structure of the Report

This report consists of 8 chapters. Chapter 1 presents the introduction of the project, followed by Chapter 2—the literature review concerning the tidal energy generation and resources assessment. In chapter 3, the tidal characteristics of different prospective areas in Indonesia, description of site selection procedures, and hydrodynamic characteristics of the chosen site are discussed. This will be followed by Chapter 4 which explains the methodology and guidelines used to assess the tidal energy resources from raw data.

Chapter 5 describes the Alas Strait model setup using POM conduct based on the method discussed in the previous chapter. In Chapter 6, the investigation and quantification of extractable tidal energy from one marine current turbine is discussed. Study to calculate the total extractable tidal energy from Alas Strait is described in chapter 7. For both chapter 6 and chapter 7, the discussion and comparison of results obtained from preceding chapter is presented at the end of each chapter. The main conclusions from this project and recommendations for further research are formulated in chapters 8 and 9 respectively.

2 LITERATURE REVIEW

2.1 Tidal Theory

Tides are the periodic change in sea level relative to the land and along coast (Gross & Gross, 1996). This is generated from the combination of gravity among the earth, the sun, and the moon. Newton's law of gravitation can be mathematically expressed as:

$$F_G = G\frac{m_1 m_2}{r^2} \quad (2\text{-}1)$$

Where F_G = Tide generating Force

G = universal gravitational constant ($6.673.10^{-11}$ Nm^2/kg^2)

m_1, m_2 = respective masses of the object (earth, sun, or moon)

r = distance between the centre of the objects

The sun has much greater mass than the moon. However, the above formula shows that the close distance between earth and the moon results in the moon to have bigger gravitational force on the ocean compared to the sun. The force causes formation of a long period wave which results in periodic changes in sea level, i.e. tides.

Tides are originally formed in the oceans and are progressing towards the coastlines, where they appear as the regular rise and fall of the sea surface. When the highest part (crest) of the wave reaches a particular location, high tide occurs; low tide corresponds to the lowest part of the wave, named as trough. The height difference between high and low tide is called tidal range.

Tide is affected by near shore hydrography, bottom friction, Coriolis acceleration, and resonant effect (Sorensen, 2006). Converging or diverging estuary shorelines causes the tidal amplitude to increase or decrease due to the concentration or spreading of tide wave's energy. The tidal range increases when tides propagate to shallower water depth; conversely it decreases due to the bottom friction which dissipates tide wave's energy.

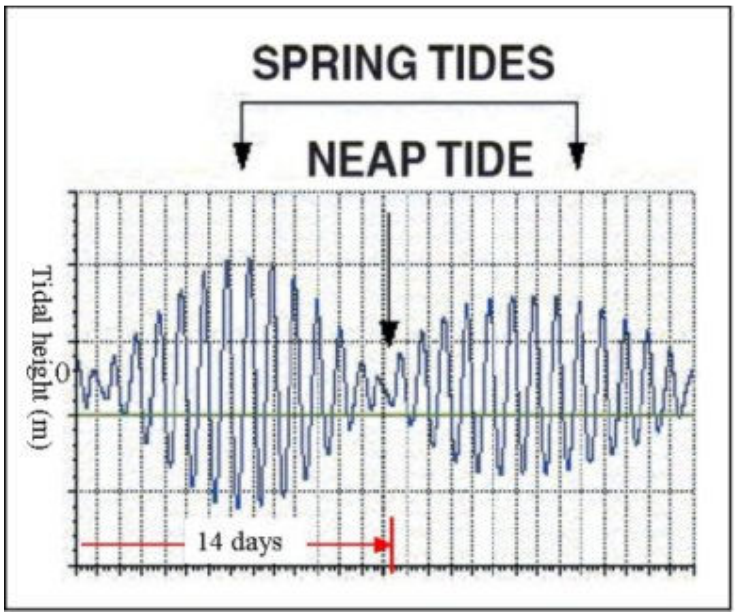

Figure 2.1: Illustration of the neap and spring tide. Source: (Energy Systems Research Unit's of The University of Strathclyde in Glasgow, 2004).

Tidal range is influenced by the relative distance and position of the earth, the sun, and the moon. Figure 2.1 shows that the tidal elevation changes every day. Spring tide is the condition when the largest tidal range occurs which happens twice a month when the gravitational pull of the sun and moon is aligned. Neap tide is the opposite of the spring tide. The ratio of springs to neaps can be as much as 2 to 1 (Russell & Macmillan, 1954).

2.1.1 Tidal Constituents

There are over 390 active tidal constituents which have periods between 8 hours to 18.6 years. Each constituent has a period, phase angle, and amplitude that depend on local condition. Most of tidal constituents are relatively small and can be neglected for practical tide prediction. In Table 2.1, eight major tidal constituents with its period, relative strength compare to M_2, and description are listed. Each constituent combines in different ways at specific location to produce the local tide. Relative strength mention in the table 2.1 below is the relative ocean response to gravitational forcing.

Table 2.1. Eight major tidal constituents. Source: (Thurman, 1997)

Symbol	Period (hours)	Relative Strength	Description
M_2	12.42	100.0	Main lunar semidiurnal constituent
S_2	12.00	46.6	Main solar semidiurnal constituent
N_2	12.66	19.1	Lunar constituent due to monthly variation in moon distance from earth
K_2	11.97	12.7	Soli-lunar constituent due to changes in declination of sun and moon throughout their orbital cycles
K_1	23.93	58.4	With O_1 and P_1 accounts for lunar and solar diurnal inequalities
O_1	25.82	41.5	Main lunar diurnal constituents
P_1	24.07	19.3	Main solar diurnal constituents
M_f	327.86	17.2	Lunar biweekly constituent

The relative importance of diurnal and semi-diurnal harmonics can be determined from ratio, F, where

$$F = \frac{K_1 + O_1}{M_2 + S_2} \tag{2-2}$$

The forms of tide may be classified as follow:

1. F = 0.00-0.25 (semi-diurnal form). Two high and low waters of approximately the same height. Mean spring tide range is $2(M_2 + S_2)$.
2. F = 0.25-1.50 (mixed, predominantly semi-diurnal). Two high and low waters daily. Mean spring tide range is $2(M_2 + S_2)$.
3. F = 1.50-3.00 (mixed, predominantly diurnal). One or two high water per day. Mean spring tide range is $2(K_1 + O_1)$.
4. F > 3.00 (diurnal form). One high water per day. Mean spring tide range is $2(K_1 + O_1)$.

2.1.2 Tidal harmonic analysis

Harmonic analysis describes the variation in water level as the summation of a constant mean level, tidal constituents, and a residual:

$$\eta = Z_0 + \sum_{i=1}^{n} a_i \cos(\Omega_i t - \phi_i) + R(t) \tag{2-3}$$

Where η = water level

Z_0 = mean water level relative to local datum

a_i = amplitude of the tidal constituents

Ω_i = frequency of the tidal constituents = $\frac{2\pi}{T_i}$

ϕ_i = phase of the tidal constituents

$R(t)$ = residual water level variation

n = number of constituents used

t = time

T_i = tidal constituents period

The minimum record required to determine main tidal constituents varies with geographical location. The accuracy of the calculations and number of tidal constituents that can be identified increases with length of record (Reeve et al., 2004).

2.1.3 Tidal current

A horizontal movement of water often accompanies the rising and falling of the tide, which is called as tidal current. The incoming tide along the coast and into the bays and estuaries is named as flood current; the outgoing tide is called ebb current. The strongest flood and ebb currents usually occur before or near the time of the high and low tides. The weakest currents occur between the flood and ebb currents and are called slack tides.

In open coast, tidal current are slow and depends on the direction of the tidal wave. However, at places where constrictions are present, the current can be rapid even when the tidal range is low (Davis Jr., 1987). In channels, the current is constrained to flow either up or down the channel. The current velocity reaches its maximum typically at halfway between high water and low water.

Tidal stream motions are constrained by the channel floor (seabed) and walls (land masses). Near the edges and the bottom, friction between the water and boundary slows the flow. Tidal stream is influenced by the shoreline bathymetry and the roughness of the surfaces. The tidal stream velocity is bigger close to the water surface,

and falls off rapidly close to the seabed. Halfway up the water column the velocity is 80% of the surface velocity (Godin, 1972). The effect of the friction to the current speed can be expressed with equation 2.4 as follow:

$$u = az^m \tag{2-4}$$

Where u = current velocity

u, m = constant

z = distance to the bottom

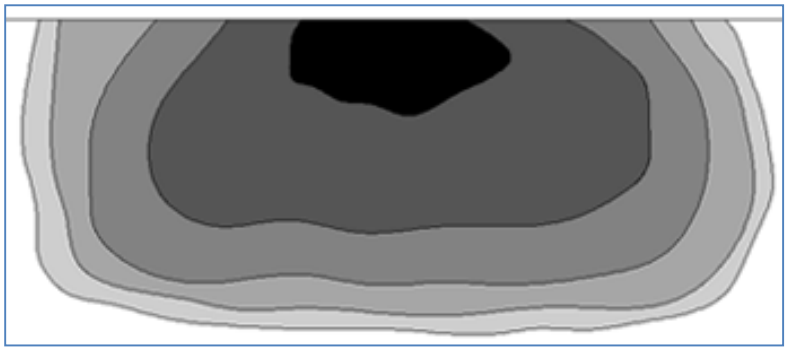

Figure 2.2: Illustration of velocity variation over cross-section of a channel. Source: (The Carbon Trust, 2009)

In figure 2.2 above, each region indicates a band of velocities, black being fastest, white is the slowest. Thus, it is clear that the flow velocity increases relative to the distance from the bottom and side boundary.

The directions of flow and the velocity profile may differ between the flood and ebb tides, the pre-dominant directions are not exactly 180° apart. Turbulence can be expected at some distance downstream of local bathymetric features (e.g. rocks, seabed shelves), and its intensity levels may be higher near the seabed.

The strength of the tidal current also fluctuates according to the tidal range. On spring tide, the tidal stream reaches its maximum. While on neap tide, the tidal stream reaches its minimum. Tidal currents can be semi-diurnal, diurnal, or mixed type, corresponding to the type of tide at the place (Charlier, 1982).

2.2 Tidal energy Extraction

The tidal energy propagates in a very long wave form. It reflects its energy at continental shelf back to the deep ocean while transporting a portion of its energy to shallow water.

There are basically two different ways to extract tidal energy. The first is by using marine current turbines, which will be explained in great details in section 2.3. The second method uses barrage scheme. The tidal barrage is a model which essentially involves a structure with gated sluices and low-head hydro turbines. Bridging two sides of an estuary, the principle of operation is to allow water to flow into the area behind the barrage with the flood tide and out during the ebb tide. As water flows out, the collected head of water turns the turbines to generate power.

There are pros and cons of using barrage scheme compared to marine current turbines (Blunden & Bahaj, 2006). One important pro is the high power density that can be focused using barrage scheme which results in a high theoretical efficiency. This has been proven to be accurate after the realisation of 240 MW tidal power barrage scheme of LaRance Barrage in Brittany, France. Whereas the cons include high capital cost, long installation time before full operation starts, and certainly the environmental problems, i.e. formation of confined water bodies which leads to changes in sediment transport distribution as well as to destruction of the water ecology. All the mentioned cons, especially the environmental problems, become the main reasons why barrage scheme is less popular than marine current turbines.

2.2.1 Advantages and disadvantages of tidal energy

Tidal energy has its own advantages and disadvantages with its implementation compared to other forms of energy. The key advantages of tidal stream energy over other forms of renewable energy, according to Bahaj & Myers (2003), are:

- High energy density**.** Since water is 830 times denser than air, flowing water contains 830 times more energy than wind blowing at the same speed. However, the exploitable range of wind speeds is much higher than tidal flows, and power is proportional to the cube of speed. Therefore, on average the energy density of tidal stream is about 4 times greater than that of wind. This means that the rotors can be smaller (and hence cheaper) than those of typical wind turbines.

- Predictable energy resource. The amount of energy and the exact time of its availability are totally predictable. This conclusion is based on the fact that the timing of high and low water and the tidal range are routinely and accurately predicted for the use of seafarers worldwide. This overcomes the intermittency problem encountered in the use of other renewable energy sources.
- The times of maximum flow rate (i.e. maximum energy resource) are sequential compared to wind and wave energy extraction, which improves the continuity of electricity supply.
- Low visual impact. Most, if not all, of the generation equipment is located underwater.

The disadvantages of tidal energy extraction compared to other renewable energy are:

- High capital cost.
- Although its energy supply can be predicted, it cannot be regulated according to the energy demand.
- Need energy conservator since its energy supply is fluctuated and can be different than the electric energy demand.

The cost to implement marine current energy is likely to decrease as new technology developed, new markets opens up, and the total installed capacity increases. This is similar with the trend in wind energy development (Bahaj & Myers, 2004).

2.2.2 Tidal energy resources assessment

Tidal energy resources assessment is usually conducted by using two different methods, flux method and the more conventional farm method.

The Flux Method can be explained as assessment methodology based on the use of solely the incoming kinetic energy flux across the front cross-sectional area of a flow channel. This method is independent of the device type, efficiency and packing density, taking only the kinetic energy flowing in the channel into account. The application of this method is most notably by Black and Veatch (2005b) for their report for Carbon Trust: “Phase II UK Tidal Stream Energy Resources Assessment”.

The major difference between both methods is the use of Significant Impact Factor (SIF) in the flux method. SIF is the percentage of the Total Resource that can be extracted without significant economic or environmental effect, to give the Available Resource.

This is site dependent. The Flux Method results in a Total Resource value for each site, which are the product of the time-varying (kinetic) power flux at a site and the cross-sectional area of the channel single.

The argument of the flux method is that clearly there is only a percentage of the total (kinetic and potential) energy in a site can be extracted without significant alteration to the flow speed. Alteration to flow speed has an important effect on the economics of energy generation in addition to possible environmental impacts. Robert Gordon University (RGU) has suggested that the percentage of this Total Resource value that is available for extraction will be dependent on the type of site. In channels where the flow is governed by a head difference at either end of the channel, significant effects of the flow can be noted when the percentage (of the kinetic energy) is around 10% (Black & Veatch, 2005a).

In the research about tidal energy flux and dissipation in continental shelf, Davies & Kwang (2000) use equation 2-5 to quantify the typical average energy flux vectors. This equation can be used to quantify the total energy flux of the flux method.

$$\left(E_x, E_y\right) = \frac{\rho_0}{T}\int_0^T \int_{-h}^{\eta} (u, v)\left[g\eta + \frac{u^2 + v^2}{2}\right] dzdt \qquad (2\text{-}5)$$

Where,

$\left(E_x, E_y\right)$ = estimated northward components of the energy flux vector

(u, v) = components of the horizontal velocity vector

η = surface elevation

ρ_0 = density

g = gravitational acceleration

The Farm Method can be explained as an extraction method based on developing an array of tidal stream devices. Each extraction has an equal amount of energy from the incoming flux. The number of devices and hence the extracted energy is purely dependent on the size of the device, its efficiency, and the packing density within the plan area. This method has been used by Bahaj & Myers (2004), Blunden & Bahaj

(2006), Energy Systems Research Unit's of The University of Strathclyde in Glasgow (2004), and Pangastuti (2005).

Steps required to carry out tidal energy resources assessment using farm method according Blunden & Bahaj (2007) are:

1. Selection of suitable sites for Marine Current Turbine (MCT) location. This depends on the current flow speed and suitable depth.
2. Determination of Initial size and type of MCT
3. Selection of the best MCT arrangement for the site
4. Investigation of the effect of MCT to the tidal downstream

Based on the above discussion of both farm method and flux, it is known that the flux method has some flaws since the SIF in this method is hard to quantify. The SIF is based on the assumption of the "acceptable" condition, while the "acceptable" itself has not been defined. Hence, it can be concluded that the use of site specific modelling as in farm method is a better choice.

Other than those common methods, Garrett and Cummins (2005) proposed that the maximum extractable average power in a channel can be calculated using equation 2-6 below.

$$P_{max} = 0.21\rho g a Q_{max} \quad (2\text{-}6)$$

Where P_{max} = maximum extractable average power

Q_{max} = maximum flow rate in the channel over period of tidal

2.3 Marine current turbines (MCT)

Advantages of tidal energy extraction with marine current turbines compared to tidal barrage are:

- As mentioned before, the technology of MCT is similar to the well-developed wind turbines technology.
- Acceptable environmental impacts (Faber Maunsell and Metro Plc., 2007) compared to the barrage scheme.

2.3.1 Problems that need to overcome with marine current turbines

To ensure the marine current turbine is installed and is functioned properly, several problems need to be encountered. According to Bahaj and Myers (2003), these problems are:

1. Operation problem. These include:
   - Corrosion. The turbines metal components need to be protected by chatodic protection, painting/coating, or using allowable thickness for corrosion.
   - Damages from debris carried by marine currents.
   - Marine growth leads to increase in dragging and hence reduce in performance
   - Harsher environmental condition, higher load.
2. Maintenance problem.
3. Installation problem, e.g. cable lying (it is proven that this problem can be encountered in oil and gas industry)
4. High axial Stresses.
5. Cavitation. Cavitation can be explained using equation 2-7 below:

$$K_f = \frac{P_{abs} - P_V}{\rho V^2/2} \qquad (2\text{-}7)$$

Where K_f = cavitations number

P_{abs} = absolute pressure

P_{hyd} = hydrostatic pressure

P_{atm} = atmospheric pressure

P_V = vapour pressure

ρ = fluid density

V = vapour pressure

K_i = inception parameter

The bigger the cavitations number, the less likely of cavitations occurrence. The inception parameter is the condition when cavitations start to occur. If cavitations number is less than inception parameter, cavitations will occur.

Other than that the fact that tidal stream extraction does not have the possibility for energy storage, unlike tidal barrage scheme (Blunden & Bahaj, 2007), should be considered in the deployment of the MCT.

2.3.2 Type of marine current turbines

Conventional tidal current turbines are classified by the position of rotor axis, i.e. mounted vertically or horizontally. Alternatively, the energy in tidal currents can be extracted by hydroplanes or harnessed indirectly, by venture devices that convert water flow into air flow, which is then used to drive the generator. The details of each type are explained in the following:

Horizontal axis turbine

Horizontal axis turbine has horizontal axis on its propeller similar to the well developed wind power turbines. The development of this technology has been significantly assisted by the development of wind turbines. This makes the horizontal axis turbine as the current leader in marine current energy installation. An example of this turbine can be seen in figure 2.3 below. This type is SeaGen model with double rotor for each pole.

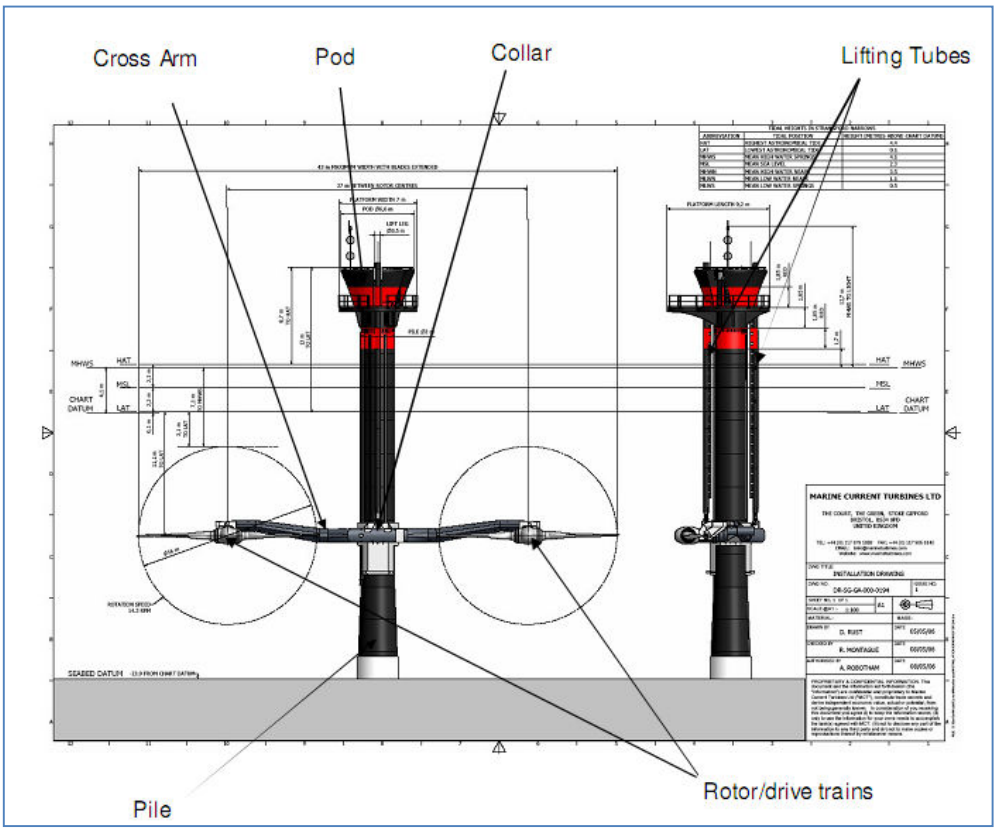

Figure 2.3: Example of horizontal axis turbines from SeaGen. Source: (Ainsworth & Thake, 2006).

The selection of rotor size and the power rating depends primarily on the depth of water where the turbine is deployed. Provided shipping can be excluded from the vicinity of the turbine installation then the rotor axis depth and the rotor diameter can be half the lowest depth of water at low tide. Examples of these turbines are SeaFlow and its newer version SeaGen (Ainsworth & Thake, 2006). These models are developed by Marine Current Turbines Ltd. with funding from the UK government.

Vertical axis turbine

The basic principle of vertical axis turbine is that near vertical blades rotate eccentrically about an axis. The resultant velocity resulting from the moving blades will generate hydrodynamic forces which provide a tangential forcing in the direction of blade movement. As long as the cumulative thrust of the blades is above a certain threshold, the blades will auto-rotate. Consequently, it is unlikely that the turbine will be able to generate enough torque to start rotation on its own. The blades can generate sufficient tangential thrust to counter blade drag if it is under rotation. So in practice, a self starting motor will be required.

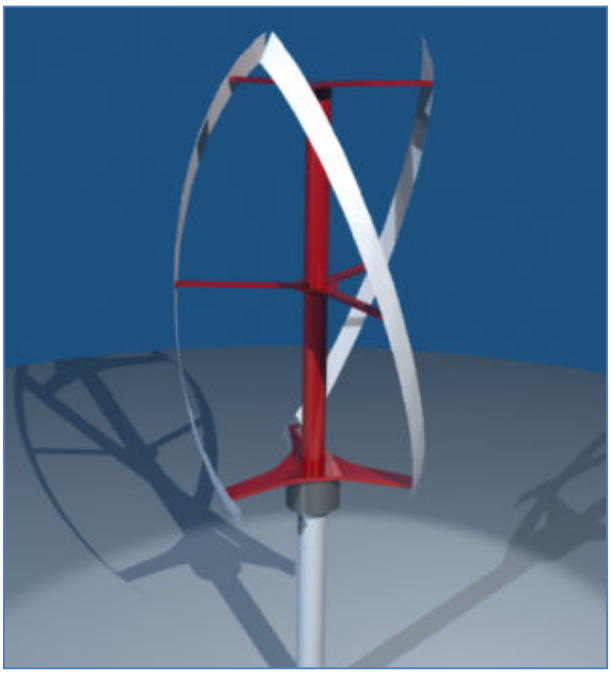

Figure 2.4: Example of vertical axis turbine using Gorlov model. Source: (Speetjens & Pittenger, 2008-2009)

However, unlike horizontal axis turbine, the vertical axis turbine has an important advantage, i.e. it requires no blade pitch control to allow for reversing of the tidal current direction. The rotor rotates at the same way irrespective of the direction of the flowing fluid. Examples of these turbines are the Davis hydro turbine (developed by Energy Inc. of Canada), the more stable Gorlov turbine (see figure 2.4 for the illustration), and Kobold turbine (produced by Enermar).

Hydrofoil Device

Oscillating hydrofoil device induces hydrodynamic lift and drag forces due to a pressure difference on the foil section caused by the relative motion of the tidal current over the foil section. These forces induce a resultant tangential force to the fixing arm by driving reciprocating hydraulic rams pump, high pressure hydraulic fluid to turn a hydraulic motor and electrical generator. Given a positive or negative angle of attack relative to the tidal stream in-flow, the hydrofoil will rise and fall in an oscillating motion. The lift which drives the device is dependent on the flow velocity and density, the foil surface area and aspect ratio and the foil profile characteristics. Examples of hydrofoil devices are the Stingray as illustrated in figure 2.5 and the SeaSnail.

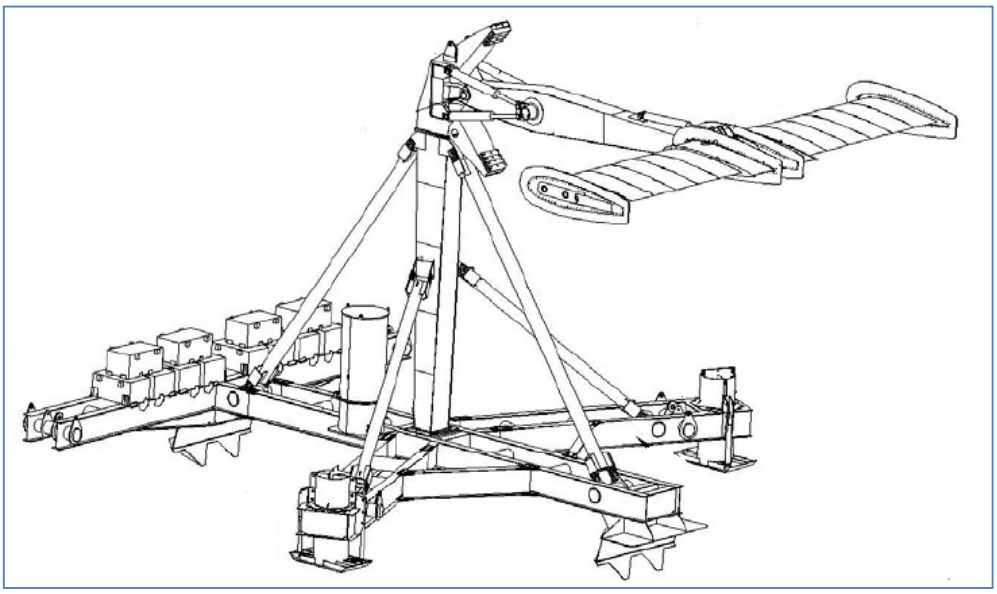

Figure 2.5: Example of hydrofoil device using Stingray model. Source: (Energy Systems Research Unit's of The University of Strathclyde in Glasgow, 2006)

Venturi Devices

The main principle of this device is utilising the static pressure drop occurring at the throat of a venturi-shaped duct which draws in air as water flows through. This air passes through a turbine, the shaft of which is connected to a generator. The advantage of this type over other tidal current turbines is that the submergible components have no moving parts, thus the turbine and generator do not need to be mounted on a surface platform. Nonetheless, a connection to the atmospheric air to the submerged components needs to be maintained. An example of this device is hydroventuri device made by Hydroventuri Ltd.

2.3.3 Assessing the power from a single turbine

Power, generated from a single turbine, can be quantified using equation 2-8 below:

$$P = C_p . A . v^3 \qquad (2\text{-}8)$$

Where P = power (Watt)

C_p = power coefficient

A = area of the turbine blade (m^2)

v = flow speed (m/s)

The power coefficient can not reach the ideal value (1), based on the Betz Law (Twidell & Weir, 2006) which states that maximum power coefficient value of 0.59. This value then has to be reduced again due to the power conversion loss, mechanical loss, angular loss, and other loss.

In their experiment using 15 m rotor with flow speed design of 2 m/s, Batten et al. (2006) conclude that the power coefficient (Cp) reaches its peak at 0.43 with pitch angle 0° and 0.35 for pitch angle 8°. Results of this experiment are illustrated in figure 2.6 below.

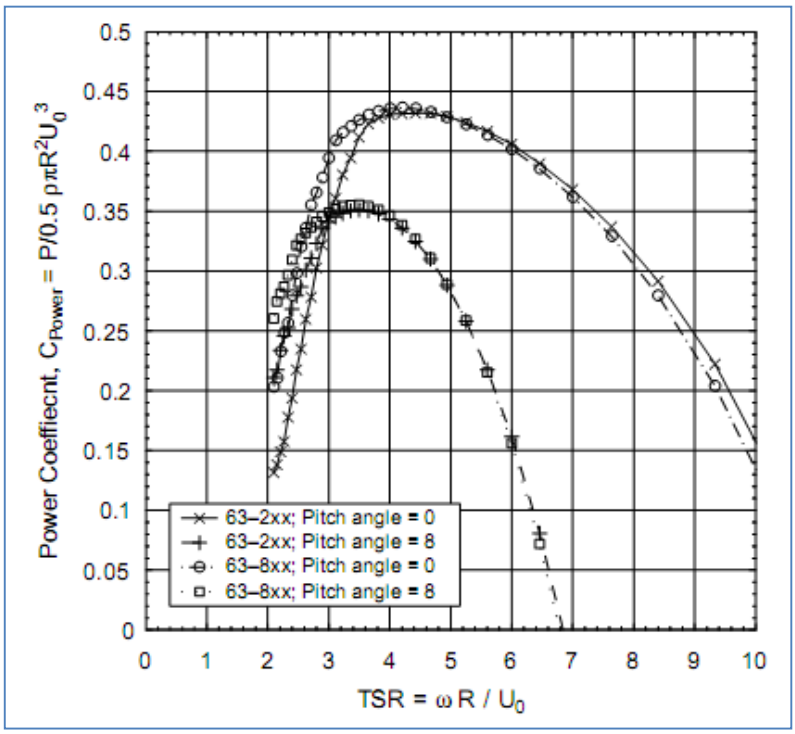

Figure 2.6: Marine current turbines rotor characteristics for two section shapes at two pitch angles (Batten et al., 2006).

This experiment is conducted by using 2 different blade designs (N.A.C.A 63-2xx and N.A.C.A 63-8xx) with two different pitch angles (0° and 8°). The rotation speed of the current is 10.9 rpm with 15 m rotor. From the figure 2.6, it can be concluded that N.A.C.A 63-8xx at pitch angle 0° is the best combination. This statement is supported by Myers (2006), who states that N.A.C.A 6-series section with high chamber is a preferable rotor section. This is resulting in promising power coefficient

The experiment results are summarised in table 2.2 below. These numbers show that power resulting from marine current turbine follows quadratic relation with the current flow speed.

Table 2.2. Typical power prediction for 15 m rotor at different flow speed. Extracted from (Batten et al., 2006).

No.	Flow speed (m/s)	Power (kW)
1	1.5	100
2	2	300
3	2.5	550
4	3	850

The value of power coefficient can also be found in the following publications.

- According to Fraenkl (1999), marine current turbines have power coefficient between 0.35-0.5.
- In Mellor (2004), C_p is varied by the flow velocity. It could reach up to 0.4-0.45. This value reaches its maximum at flow speed between 1.75 to 3.5 m/s.
- Result from the SeaFlow Project, value of $C_p \approx 0.4$ (Thake, 2005).
- Power output from typical 15m diameter turbine with Cp=0.3 results in average power of 300 kW (Blunden & Bahaj, 2006).

2.3.4 Tidal array configuration

The turbines in array are expected to be arranged in row of 10 to 20 rotor diameters apart (Bahaj & Myers, 2004).

In accordance with Bahaj and Myers (2004), tidal array depends on three parameters, i.e. depth, width, and length. In their resources assessment in 2005, Myers and Bahaj, set the limit for a tidal array configuration as follow:

Depth

Tidal turbine critical depth—depth where large changes in flow speed occurs which may cause disruption to the operation– is set based on equation 2-9. This is essential since wave can disrupt upper portion of the flow and increase loading to the turbines.

$$Dc = \left(\frac{(AV)^2}{gB^2}\right)^{1/3} \quad (2\text{-}9)$$

Where: Dc = critical depth

A = cross sectional area of the channel

V = flow velocity

B = breadth of the channel

The lowest blade point swept is expected to be at least ¼ times depth (Bahaj & Myers, 2004).

Width

The width between tidal turbines has to be regulated to neglect the effect of wake expansion downstream of the devices. The width is also to be regulated to provide a sufficient quantity of free stream fluids to pass between rotors, to reduce blockage effect and promote fluid mixing. According to Myers (2006), the lateral spacing of 3 times diameter between blade tips taken for each row leads to reduction in flow speed approximately 12%.

Length

Myers (2006) suggests setting the minimum distance between arrays as 15 times the diameter of the turbines. Whilst Myers and Bahaj (2005), use 200 m as the lateral distance between sub-arrays and 500 m as the longitudinal distance between arrays. This space is needed for ship transportation and MCT maintenance.

Equation 2-10 can be used to calculate the downstream flow velocity after tidal array. Assumption for this equation: flow is fully mixed when it encounters the devices row.

$$U_{dr} = \left|\frac{A_b}{A_{total}}(1-2a) + \frac{A_{free}}{A_{total}}\right| U_0 = R_{DF}U_0 \quad (2\text{-}10)$$

Where a = rotor axial induction factor

U_{dr} = Downstream flow velocity

A_b = sub-array area occupied by rotor (blockage)

A_{free} = cross sectional area of free rotors

A_{total} = total cross sectional area of the sub-array

R_{DF} = raw velocity decay factor

With the array reach its maximum efficiency at a = 1/3 (Burton et al., 2001).

Electrical connection of the array

For near shore locations (less than 10 km from the coast), it is preferable to link individual MCT transformer to an onshore transformer station using low voltage cable. Whilst for offshore locations (more than 10 km from the coast), it is preferable to link individual MCT to an offshore transformer station (Myers & Bahaj, 2005).

2.4 Princeton Ocean Model (POM)

2.4.1 Introduction to POM

POM (Princeton Oceanic Model) is a numerical model based on a three-dimensional primitive equation, time dependent sigma coordinate, free surface, and coastal ocean circulation model (Blumberg & Mellor, 1987). The principal attributes of POM are:

- The vertical grid is based on sigma coordinate (terrain-following) model, which means that the water column is divided into an equal number of relative vertical layers regardless of the depth.
- The horizontal grid uses curvilinear orthogonal coordinates and “Arakawa C” differencing scheme.
- It contains imbedded second moment turbulence closure sub-model to provide vertical mixing coefficient.
- An explicit time step is used for horizontal differencing, and implicit scheme is used for vertical differencing. Combination of both steps enables the use of fine vertical resolution in the surface and shallow layers.
- The model implements a complete thermodynamics scheme (Mellor & Yamada, 1985).
- The model has a free surface and a split time step. The internal mode is three-dimensional and uses a long time step based on CFL (Courant-Friedrich-Lewy) condition and internal wave speed. The external mode is two-dimensional and uses a short time step based on CFL condition and external wave speed.

POM is written in standard Fortran 77 language. The latest version of POM to date is POM08. This version is a combination of POM2K and wetting and drying function.

2.4.2 Basic equations

The basic equation in POM is slightly different than other CFD program since it uses sigma coordinate system. The sigma coordinate system illustration can be seen in figure 2.7 below.

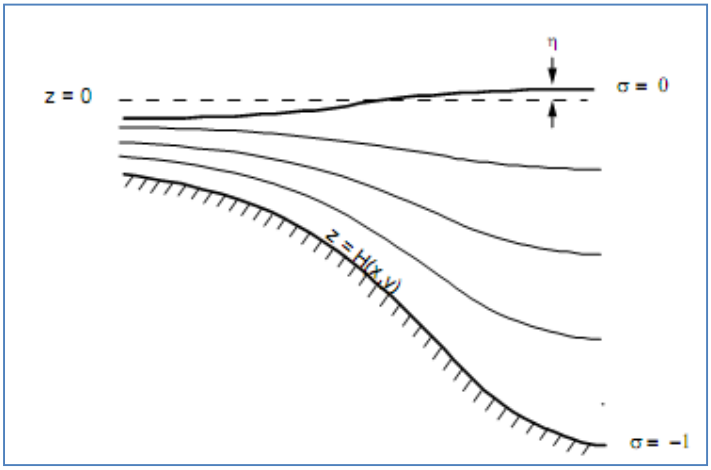

Figure 2.7: Typical sigma coordinate (Mellor, 2004)

Sigma coordinate equations are based on the following transformation (equation 2-11 to equation 2-15):

$$x^* = x \tag{2-11}$$

$$y^* = y \tag{2-12}$$

$$\sigma = \frac{z - \eta}{H + \eta} \tag{2-13}$$

$$t^* = t \tag{2-14}$$

$$D \equiv H + \eta \tag{2-15}$$

Where x, y, z = conventional Cartesian coordinates

$\eta(x, y, t)$ = surface elevation

H = bottom depth (in meter)

t = time (in second)

Sigma (σ) ranges from $\sigma = 0$ at $z = \eta$ to $\sigma = 1$ at $z = \eta$

The basic equation for POM can be summarised as equation 2-16 through equation 2-22. These equations are based on horizontal Cartesian coordinate.

$$\frac{\partial DU}{\partial x} + \frac{\partial DV}{\partial y} + \frac{\partial \omega}{\partial \sigma} + \frac{\partial \eta}{\partial t} = 0 \tag{2-16}$$

$$\begin{aligned} &\frac{\partial UD}{\partial t} + \frac{\partial U^2 D}{\partial x} + \frac{\partial UVD}{\partial y} + \frac{\partial U\omega}{\partial \sigma} - fVD + gD\frac{\partial \eta}{\partial x} \\ &\quad + \frac{gD^2}{\rho_0}\int_\sigma^0 \left[\frac{\partial \rho'}{\partial x} - \frac{\sigma'}{D}\frac{\partial D}{\partial x}\frac{\partial \rho'}{\partial \sigma'}\right] d\sigma' \\ &\quad = \frac{\partial}{\partial \sigma}\left[\frac{K_M}{D}\frac{\partial U}{\partial \sigma}\right] + F_x \end{aligned} \tag{2-17}$$

$$\begin{aligned} &\frac{\partial VD}{\partial t} + \frac{\partial UVD}{\partial x} + \frac{\partial V^2 D}{\partial y} + \frac{\partial V\omega}{\partial \sigma} + fUD + gD\frac{\partial \eta}{\partial y} \\ &\quad + \frac{gD^2}{\rho_0}\int_\sigma^0 \left[\frac{\partial \rho'}{\partial y} - \frac{\sigma'}{D}\frac{\partial D}{\partial y}\frac{\partial \rho'}{\partial \sigma'}\right] d\sigma' \\ &\quad = \frac{\partial}{\partial \sigma}\left[\frac{K_M}{D}\frac{\partial V}{\partial \sigma}\right] + F_y \end{aligned} \tag{2-18}$$

$$\frac{\partial TD}{\partial t} + \frac{\partial TUD}{\partial x} + \frac{\partial TVD}{\partial y} + \frac{\partial T\omega}{\partial \sigma} = \frac{\partial}{\partial \sigma}\left[\frac{K_H}{D}\frac{\partial T}{\partial \sigma}\right] + F_T - \frac{\partial R}{\partial z} \tag{2-19}$$

$$\frac{\partial SD}{\partial t} + \frac{\partial SUD}{\partial x} + \frac{\partial SVD}{\partial y} + \frac{\partial S\omega}{\partial \sigma} = \frac{\partial}{\partial \sigma}\left[\frac{K_H}{D}\frac{\partial S}{\partial \sigma}\right] + F_R \tag{2-20}$$

$$\begin{aligned} &\frac{\partial q^2 D}{\partial t} + \frac{\partial Uq^2 D}{\partial x} + \frac{\partial Vq^2 D}{\partial y} + \frac{\partial \omega q^2}{\partial \sigma} \\ &\quad = \frac{\partial}{\partial \sigma}\left[\frac{K_q}{D}\frac{\partial q^2}{\partial \sigma}\right] + \frac{2K_M}{D}\left[\left(\frac{\partial U}{\partial \sigma}\right)^2 + \left(\frac{\partial V}{\partial \sigma}\right)^2\right] \\ &\quad + \frac{2g}{\rho_0}K_H\frac{\partial \tilde{\rho}}{\partial \sigma} - \frac{2Dq^3}{B_1 l} + F_q \end{aligned} \tag{2-21}$$

$$\frac{\partial q^2 lD}{\partial t} + \frac{\partial U q^2 lD}{\partial x} + \frac{\partial V q^2 lD}{\partial y} + \frac{\partial \omega q^2 l}{\partial \sigma} = \frac{\partial}{\partial \sigma}\left[\frac{K_q}{D}\frac{\partial q^2 l}{\partial \sigma}\right] + E_1 l\left(\frac{K_M}{D}\left[\left(\frac{\partial U}{\partial \sigma}\right)^2 + \left(\frac{\partial V}{\partial \sigma}\right)^2\right] + E_3 \frac{g}{\rho_0} K_H \frac{\partial \tilde{\rho}}{\partial \sigma}\right) - \frac{Dq^3}{B_1}\tilde{W} + F_l \quad (2\text{-}22)$$

Where U = horizontal flow velocity in x-direction (m/s)

V = horizontal flow velocity in y-direction (m/s)

W = vertical velocity in z-direction (m/s)

ω = sigma coordinate vertical velocity (m/s)

f = Coriolis parameter (s^{-1})

g = acceleration of gravity (m/s^2)

ρ = water density (kg/m^3)

K_M = vertical kinematic velocity (m^2/s)

K_H = vertical diffusivity

A_M = horizontal kinematic velocity (m^2/s)

A_H = horizontal heat diffusivity

q^2 = two times the turbulent kinetic energy (m^2/s^2)

l = turbulent length scale (m)

T = potential temperature (K)

S = salinity (psu)

R = short wave radiation flux (m.K/s)

The transformation to the Cartesian velocity is:

$$W = \omega + U\left(\sigma\frac{\partial D}{\partial x} + \frac{\partial \eta}{\partial x}\right) + V\left(\sigma\frac{\partial D}{\partial y} + \frac{\partial \eta}{\partial y}\right) + \sigma\frac{\partial D}{\partial t} + \frac{\partial \eta}{\partial t} \quad (2\text{-}23)$$

The horizontal viscosity and diffusion equation are defined with:

$$F_x \equiv \frac{\partial}{\partial x}(H\tau_{xx}) + \frac{\partial}{\partial y}(H\tau_{xy}) \quad (2\text{-}24)$$

$$F_y \equiv \frac{\partial}{\partial x}(H\tau_{xy}) + \frac{\partial}{\partial y}(H\tau_{yy}) \quad (2\text{-}25)$$

With

$$\tau_{xx} = 2A_M\frac{\partial U}{\partial x}\ ;\ \tau_{xy} = \tau_{yx} = A_M\left(\frac{\partial U}{\partial y} + \frac{\partial V}{\partial x}\right)\ ;\ \tau_{yy} = 2A_M\frac{\partial V}{\partial y} \quad (2\text{-}26)$$

Also,

$$F_\phi \equiv \frac{\partial}{\partial x}(Hq_x) + \frac{\partial}{\partial y}(Hq_y) \quad (2\text{-}27)$$

With

$$q_x \equiv A_H\frac{\partial \phi}{\partial x}\ ;\ \ q_y \equiv A_H\frac{\partial \phi}{\partial y} \quad (2\text{-}28)$$

Where ϕ represents T, S, q^2, or $q^2 l$.

Where A_M, the vertically integrated horizontal eddy viscosity is defined by the Smagorinsky formula:

$$A_M = C\ \Delta x\ \Delta y\frac{1}{2}|\nabla V + (\nabla V)^T| \quad (2\text{-}29)$$

With,

$$|\nabla V + (\nabla V)^T| = \left[\left(\frac{\partial u}{\partial x}\right)^2 + \frac{\left(\frac{\partial v}{\partial x} + \frac{\partial u}{\partial y}\right)^2}{2} + \left(\frac{\partial v}{\partial y}\right)^2\right]^2 \quad (2\text{-}30)$$

Where C = Horcon parameter (non-dimensional)

Δx = grid spacing in x direction

Δy = grid spacing in y direction

Equation for the surface elevation is:

$$\frac{\partial \eta}{\partial t} + \frac{\partial \bar{U} D}{\partial x} + \frac{\partial \bar{V} D}{\partial y} = 0 \tag{2-31}$$

After the integration of the surface elevation equation, the momentum equations become:

$$\frac{\partial \bar{U} D}{\partial t} + \frac{\partial \bar{U}^2 D}{\partial x} + \frac{\partial \bar{U}\bar{V} D}{\partial y} - \tilde{F}_x - f\bar{V}D + gD\frac{\partial \eta}{\partial x} = -< wu(0) > + < wu(-1) > + G_x - \frac{gD}{\rho_0}\int_{-1}^{0}\int_{\sigma}^{0}\left[D\frac{\partial \rho'}{\partial x} - \frac{\partial D}{\partial x}\sigma'\frac{\partial \rho'}{\partial \sigma}\right]d\sigma' d\sigma \tag{2-32}$$

$$\frac{\partial \bar{V} D}{\partial t} + \frac{\partial \bar{U}\bar{V} D}{\partial x} + \frac{\partial \bar{U}^2 D}{\partial y} - \tilde{F}_y - f\bar{U}D + gD\frac{\partial \eta}{\partial y} = - < wv(0) > + < wv(-1) > + G_y - \frac{gD}{\rho_0}\int_{-1}^{0}\int_{\sigma}^{0}\left[D\frac{\partial \rho'}{\partial y} - \frac{\partial D}{\partial y}\sigma'\frac{\partial \rho'}{\partial \sigma}\right]d\sigma' d\sigma \tag{2-33}$$

Where $< wu(0) >, < wv(0) >$ = momentum fluxes at the surface (m^2/s^2)

$< wu(0) >, < wv(0) >$ = momentum fluxes at the bottom (m^2/s^2)

Vertically integrated velocities ($\bar{U}$) are defined with:

$$\bar{U} \equiv \int_{-1}^{0} U\, d\sigma \tag{2-34}$$

The quantities of $\tilde{F}_x$ and $\tilde{F}_y$ are defined according to:

$$\tilde{F}_x = \frac{\partial}{\partial x}\left[H2\bar{A}_M\frac{\partial \bar{U}}{\partial x}\right] + \frac{\partial}{\partial y}\left[H\bar{A}_M\left(\frac{\partial \bar{U}}{\partial y} + \frac{\partial \bar{V}}{\partial x}\right)\right] \tag{2-35}$$

$$\tilde{F}_y = \frac{\partial}{\partial y}\left[H2\bar{A}_M\frac{\partial \bar{V}}{\partial y}\right] + \frac{\partial}{\partial x}\left[H\bar{A}_M\left(\frac{\partial \bar{U}}{\partial y} + \frac{\partial \bar{V}}{\partial x}\right)\right] \tag{2-36}$$

The dispersion terms are defined according to:

$$G_x = \frac{\partial \overline{U}^2 D}{\partial x} + \frac{\partial \overline{U}\overline{V} D}{\partial y} - \tilde{F}_x - \frac{\partial \overline{U^2} D}{\partial x} - \frac{\partial \overline{UV} D}{\partial y} + \bar{F}_x \quad (2\text{-}37)$$

$$G_y = \frac{\partial \overline{U}\overline{V} D}{\partial x} + \frac{\partial \overline{V}^2 D}{\partial y} - \tilde{F}_y - \frac{\partial \overline{UV} D}{\partial x} - \frac{\partial \overline{V^2} D}{\partial y} + \bar{F}_y \quad (2\text{-}38)$$

The curvature term, $\tilde{f}$, can be defined with:

$$\tilde{f} = \frac{V\delta_x(\Delta y)}{\Delta x \Delta y} + \frac{U\delta_y(\Delta x)}{\Delta x \Delta y} \quad (2\text{-}39)$$

The quadratic law with bottom friction coefficient, C_b, is used for bottom friction (τ_b^x, τ_b^y):

$$\tau_b^x = C_b \sqrt{U^2 + V^2} U \quad (2\text{-}40)$$

$$\tau_b^y = C_b \sqrt{U^2 + V^2} V \quad (2\text{-}41)$$

At the open boundary, tidal elevations for each tidal constituent are defined as

$$h_i(t) = \gamma A_i \cos(\varpi t + E - \theta_i) \quad (2\text{-}42)$$

Where i = index of the model grid along the open boundary

h = tidal elevation along the open boundary

γ = node factor

A_i = tidal constituent amplitude

θ_i = epoch

ϖ = angular speed

E = value of equilibrium when t = 0.

2.4.3 The advantages and disadvantages of POM

As compared to other CFD (Computational Fluid Dynamics) programs, POM has some advantages (Ezer et al., 2002). These advantages include:

- Best suited for modelling regional coastal simulation since it is suitable for modelling flows over continental shelf and slope.

- Can produce a smooth representation of the topography.
- Suitable in situation where capturing the dynamical and/or boundary layer effect associated with topography is important. POM with sixth order combined compact difference scheme gives smallest barothrophic velocity error compare d to other sigma models.

Nevertheless, it also has some known weaknesses:

- Not able to produce good approximations in modelling in global coupled climate modelling context. (Griffies et al., 2000)
- may have numerical error in pressure gradient calculations over steep topography (Ezer et al., 2002)

2.4.4 Boundary condition in POM

There are two types of boundary conditions in POM, closed boundary condition and open boundary condition (OBC). The closed boundary condition consists of land masses in the horizontal direction and bottom of the sea in vertical direction. In closed boundary condition, the fluid flow is restricted.

Meanwhile, the fluid motion should be unrestricted in open boundaries. There are two types of OBC, passive type (where information pass boundary condition without reflection), and active type (where the boundary is used to drive the simulation).

POM uses mode splitting technique, vertically averaged velocities and free surface elevation (external mode) are calculated with shorter time step compared to depth-varying variables in internal mode (Carter & Merrifield, 2007).

External Mode in POM

There are three variables to be solved (water elevation, x-direction and y-direction flow velocity) with only one variable defined. Zero gradient is used (Φ_b = Φ of interior neighbour).

Boundary conditions used for tidal simulations include:

- Clamped elevation. Free surface displacement set to an externally prescribed value.

$$\eta_{b\pm1} = \eta^{ext} \quad (2\text{-}43)$$

- Clamped normal velocity. Horizontal velocity is set to an externally prescribed value. This value can be obtained from survey or other model.

$$V_{n,b} = V_n^{-ext} \quad (2\text{-}44)$$

- Flather condition. Applied and adjusted externally prescribed normal velocity based on the difference between modelled and externally prescribed surface elevation.

$$V_{n,b} = V_n^{-ext} \pm \sqrt{\frac{g}{H}}(\eta_{b\pm1} - \eta^{ext}) \quad (2\text{-}45)$$

Flather condition gives more accurate result than clamped condition.

Internal mode in POM

There are depth varying variables within POM. These are the three velocity components (u, v, w), temperature, salinity, turbulent kinetic energy, and turbulent length scale.

In the internal mode the OBC should fulfil:

1. It does not reflect the energy back to the interior domain when a range of vertical modes are present.
2. Realistic topography is included in the boundary condition
3. Kinetic and potential energy are treated similarly
4. No additional horizontal viscosity is added in the boundary region

Modified flow relaxation scheme is best suited for above criteria. The flow relaxation scheme equation in POM can be represented with equation 2-46 below. This scheme is designed to absorb the outgoing energy in the boundary condition.

$$\phi = \alpha\phi^{ext} + (1-\alpha)\phi^{*} \quad (2\text{-}46)$$

Where ϕ^{*} = time integrated value calculated by the model

α = relaxation number (varies from 0 to 1).

For POM, it is very important to use smoothing on the open boundary parameter vector. Without smoothing, POM can be integrated only with a certain period and will blow up afterward. According to Chu et al (1997), the use of smoothing results in a computationally stable model.

3 STUDY AREA AND SITE SELECTION

3.1 Tidal Characteristics in Indonesia

In figure 3.1 below, tidal constituents in 96 locations in Indonesia are presented. These data are the official data obtained from Indonesian Navy. As shown in the map, tidal constituents height is varied across Indonesia with the maximum located in the South of Papua Island, the east-most location in Indonesia.

Locations in northern part of Sumatra Island (west Indonesia) are mostly dominated by semi-diurnal tides, whilst in the south-eastern part are dominated by diurnal tides. The highest tide in western part of Indonesia is located in the area near Malacca Strait, in between the small islands.

For locations in central Indonesia the tide is mixed with predominantly semi-diurnal in northern part of Kalimantan and Sulawesi, while mixed predominantly diurnal occurs in southern part of Kalimantan and Sulawesi, Java, Bali and Lombok. In east Indonesia, the tide is mixed similar to that in central part of Indonesia with predominantly semidiurnal in northern part and predominantly diurnal for most of the southern part.

In conclusion, tidal characteristics in Indonesia are mainly mixed but dominated by semi-diurnal tide. However, In Java Sea, the diurnal tide is more dominant than semi-diurnal tide, in contrast with both Pacific and Indian Ocean (Koropitan & Ikeda, 2008).

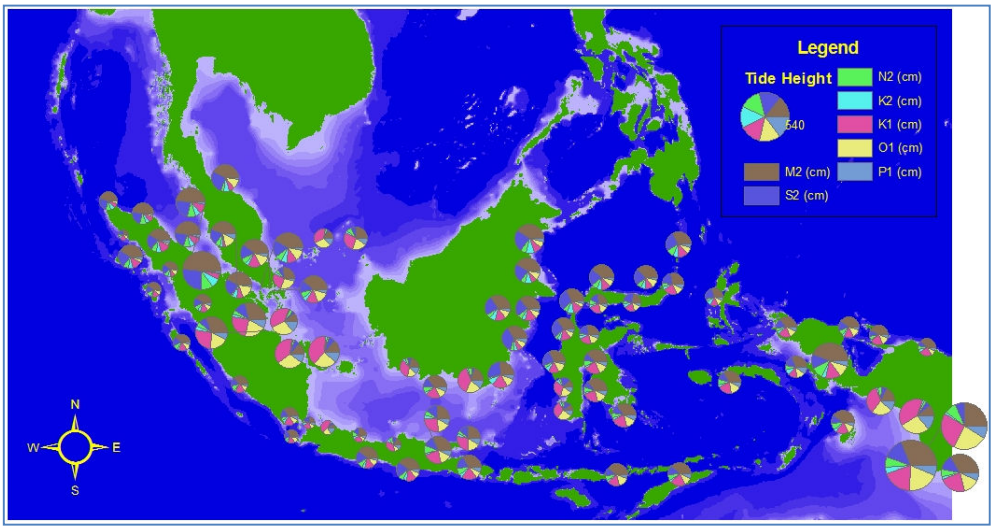

Figure 3.1: Tidal constituents in Indonesia (unit in cm). Extracted from Hydro-Oceanographic Service Indonesian Navy (2009a).

In addition to tidal constituents, Hydro-Oceanographic Service of Indonesian Navy also issues documents that show current velocity in 18 locations in Indonesia, which are summarised in figure3.2. Since most of the sites shown are located in Malacca Strait, and do not cover most of the potential tidal energy location in Indonesia, these data cannot be the only source for site selection.

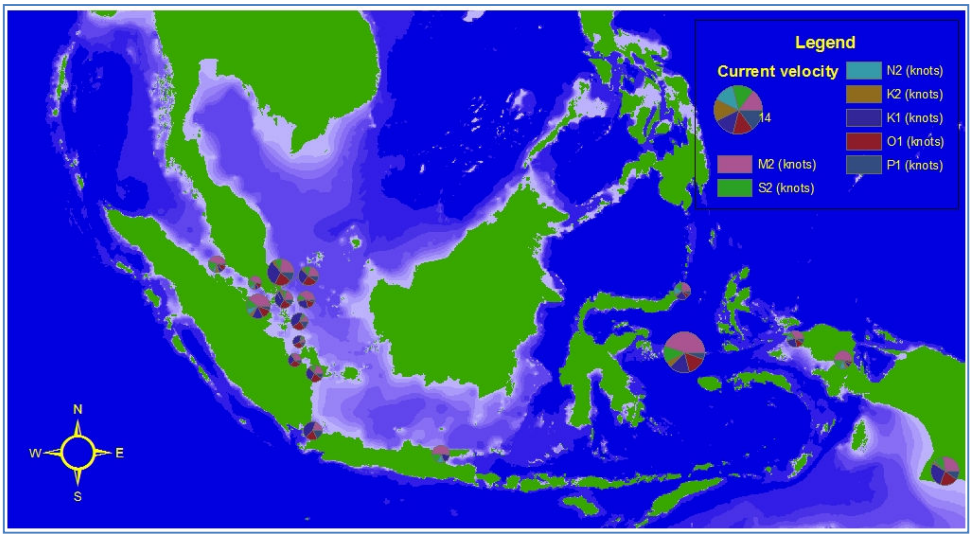

Figure 3.2: Tidal current velocity in Indonesia (unit in m/s). Extracted from Hydro-Oceanographic Service Indonesian Navy (2009b).

The recorded data of tidal constituents in Indonesia are mostly located in harbour and navigational channel. Unfortunately, there are many places without any record at all. For these places, global tidal model is highly important to produce a good approximation of data. The global tidal model for Indonesia created by Egbert and Erofeeva (2009) can be seen in figure 3.3 and figure 3.4 below.

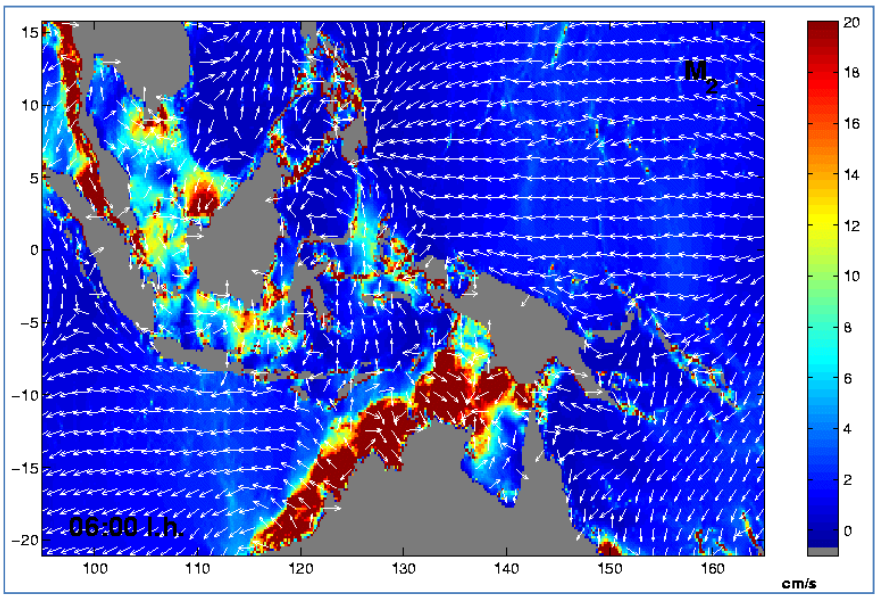

Figure 3.3: Indonesia inverse tidal solution (ITS) for M2 tidal currents at 06.00 h. Source: (Egbert & Erofeeva, 2009).

This model confirms all conclusions from figure 3.1 and 3.2. By comparing figure 3.3 and figure 3.4, it is clearly shown that in Java Sea the predominant tide is diurnal. In Malacca Strait, semi-diurnal is the predominant tide. In addition, the model validates that the biggest open ocean tidal range and the biggest open ocean tidal current are in the same location, i.e. in the southern part of Papua Island.

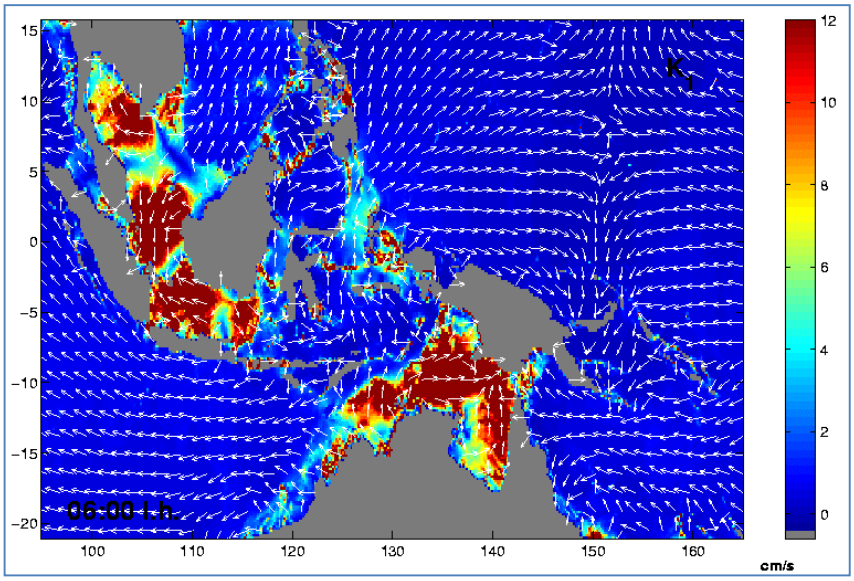

Figure 3.4: Indonesia inverse tidal solution (ITS) for K1 tidal currents at 06.00 h. Source: (Egbert & Erofeeva, 2009).

3.2 Site Selection

3.2.1 Criteria for Site Selection

The criteria for site selection in this project are acquired from the similar projects conducted in all over the world. These criteria include:

- High current velocity. The minimum flow velocity for economic deployment of marine current energy is 1 m/s (EU Commission, 1996).
- Adequate water depth. According to Myers and Bahaj (2005), if the depth is too shallow i.e. less than 25 m, the diameter of the turbine will be too small thus it is not economically feasible. However, if the water too deep (more than 45 m), the installation will be a problem.
- The location needs to be wide enough for sets of tidal array to be installed.
- The location is not a major shipping lane. Since Indonesia is located between two continents and between two oceans, it becomes a major shipping lane from Asia to Europe and Africa. Therefore, some potential locations cannot be considered (e.g. Malacca Strait).
- The location must be near to the existing electricity grid. This criteria is based on the fact marine current turbine energy is highly dependent on the intensity of the current; hence it is difficult to regulate and to conserve. Therefore, it will be more economically efficient if the excess of energy generated is distributed directly to the electricity grid. This means that remote area (e.g. straits and waters around Papua Island) cannot be considered.

In addition to the above criteria, Black & Veatch (2005) concludes that the best prospective sites for tidal energy installation are sites with flow velocity higher than 2.5 m/s with depth more than 30 m. This statement is based on the comparison of cost, performance, and unit energy cost ($/kWh). It also concludes that floating turbine is preferable for a site with depth more than 40 m, whilst seabed standing turbine is suitable for a site with depth between 30-40 m.

3.2.2 Difficulties in Selecting Site

As mentioned briefly in chapter 1, there are many obstacles in choosing a specific site to assess its tidal energy resource. In fact, a lot of sites that fulfil most of the criteria for site selection are lack of data.

Since the velocity is highly dependent on the bathymetry, an accurate bathymetric map or navigational map is very important in modelling the area. Without a local bathymetric map, the highest resolution map available is from GEBCO 2008 map, which has resolution of 1 minute grid. However, its accuracy is not sufficient for modelling narrow channel between islands.

One crucial step in selecting site is the final calibration for the completed model, which requires either tidal height data or tidal current data. Nonetheless, these data are extremely rare in all over Indonesia.

3.2.3 Selecting Site

Considering the last three criteria for site selection, it can be concluded that some of the apparent site cannot be selected. These sites include Malacca Strait, waters around Papua, Straits in Maluku and the straits in between small islands.

Schiller (2004) creates a flow model for tidal stream condition in Indonesia, that uses x-direction grid size of 0.5°, y-direction grid size of 0.33° and 36 vertical levels. This model incorporates wind stress, surface heat flux, and short wave radiation as the surface forcing. The model can be seen in figure 3.5 below.

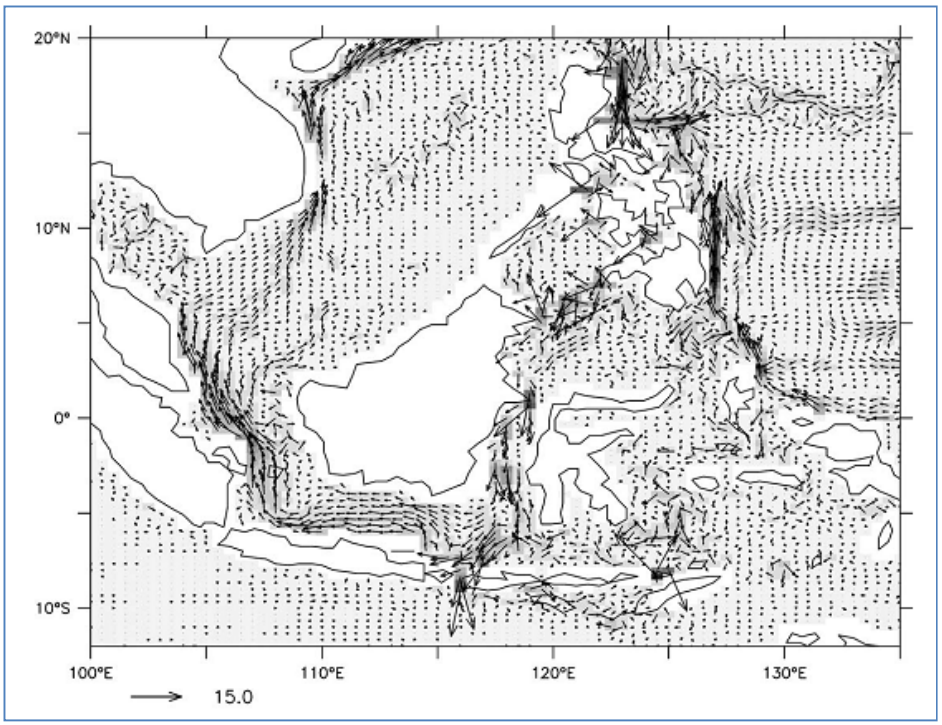

Figure 3.5: Mean tidal residual currents (barotropic) in the Indonesian Seas. Units are in cm/s. Source: (Schiller, 2004).

This model and both models illustrated in figure 3.3 and 3.4 can be used as guidelines for selecting high current velocity site in Indonesia. However, these studies have limitations: (1) the grid cell is coarse resolution, (2) the whole area is assumed to have the same depth or in other words, no bathymetry chart is used, (3) use the global constant for the value of tidal frequency and amplitude for all locations.

Based on the above discussion, it is found that out of all the areas presented in figure 3.3 to 3.5 only Lombok Strait, Alas Strait, and Makassar Strait able to fulfil all the criteria for site selection. Considering the bathymetry of the three sites, it is known that the water depth in Lombok Strait and Makassar Strait are too deep for tidal turbine installation. Therefore, it can be concluded that the most appropriate site is the Alas Strait.

The summary of site comparison in Indonesia with respect to the site selection criteria is presented in table 3.1 below. The positive sign (+) represents a site that fulfils the criteria, whilst the negative sign (-) is used for site which fails the criteria.

Table 3.1. Summary of tidal energy site selection in Indonesia

Site	Current velocity	Water depth	Site width	No major shipping lane	Electricity grid	Availability of data
Malacca Strait	+	+	+	-	+	+
Lombok Strait	+	-	+	+	+	+
Alas Strait	+	+	+	+	+	+
Sunda Strait	-	-	+	+	+	+
Makassar Strait	-	-	+	+	+	+
Capalulu Strait	+	-	-	+	-	-
Berau Bay	+	+	+	+	-	+

3.3 Alas Strait Characteristics

The Alas Strait is a strait connecting Lombok Island and Sumbawa Island. The strait has 50 km length, in the north-south direction. The width is varied from 16 km in its narrowest location to 30 km in its widest location. The depth of the strait is varied from

around 15 meter in the area near to the coastline to the deepest part in the middle around 180 m. Its location relatives to Indonesia can be seen in figure 3.6.

Figure 3.6: Alas Strait.

The Alas Strait belongs to the deep water ocean category with rocky and sandy at the bottom. Alas Strait is also, with Lombok Strait, crossed by the Indonesian through flow from and to Indian Ocean and Java Sea.

4 METHODOLOGY

4.1 Data Collection

The data needed for conducting tidal energy resources assessment are bathymetry map, tidal constituent data (amplitude and phase), and tidal stream data for calibrating the results.

4.1.1 Bathymetry Map

The bathymetric map used is the bathymetric chart of Alas Strait (map no.293, edition 2006) from DISHIDROS TNI-AL (Hydro-Oceanographic Division of Indonesian Navy). The scale of this map is 1:200000. The depth is showed in meter from the datum which is the lowest normal for low water. This map is using Mercator projection with World Geodetic System 1972 spheroid. The region limit of the map is 19°15' S - 8°05' S, 116°21' E - 117°35' E. The map can be seen in figure 4.1 below.

Figure 4.1: Alas Strait Bathymetric Map

4.1.2 Tide Data

The tidal constituents used in this model are obtained using OTIS from "Indonesian Seas Inverse Tidal Solution" (Egbert & Erofeeva, 2009). OTIS is a package of programs for tidal data assimilation based on methods used by Egbert et al. (1994) and Egbert and Erofeeva (2002). The model, "I*ndonesian Seas Inverse Tidal Solution*", is the current version of Indonesian model of ocean tides, which best-fits, in a least-squares sense, the Laplace Tidal Equations and along track averaged data from TOPEX/Poseidon.

The tides are provided as complex amplitudes of earth-relative sea-surface elevation for eight primary (M_2, S_2, N_2, K_2, K_1, O_1, P_1, Q_1) harmonic constituents, on a 420x220 grid, 1/6 degree resolution full global grid. Region limits for this model are 21° S - 15.66667° N, 95° E - 165° E. Topography used in this model are Gtopo30 (Smith & Sandwell, 1997). It has 5880 Topex/Poseidon data sites. According to Egbert and Erofeeva (2002) the posterior error for tidal constituent M2 and K1 at sites around Alas Strait could reach 2-4 cm.

4.1.3 Tidal stream data

The tidal stream data for calibrating the model are acquired from the survey report by Kobold Nusa (2008). This report is intended to support the renewable energy program by Indonesia's Ministry of research and technology.

The measurement are taken in two nearby locations in offshore of East Lombok. The duration of the measurement is thirty days with twenty minutes interval. This survey uses 2 types of ADCP (Accoustic Doppler Current Profiler), Agronaut dan Nortek Continental.Other than calculating the current speed, the survey also observes the bathymetry and characteristics of the area for its suitablility for tidal stream generation. The locations of the survey in Tanjung Menangis can be seen from the figure 4.2 below.

Figure 4.2: Location of the tidal stream survey

4.2 Assessment Method

The tidal energy resources assessment method for Alas Strait is to combine the previous examples by Blunden and Bahaj (2006), Myers and Bahaj (2005), and Pangastuti (2005). This method can be summarised as figure 4.3 below.

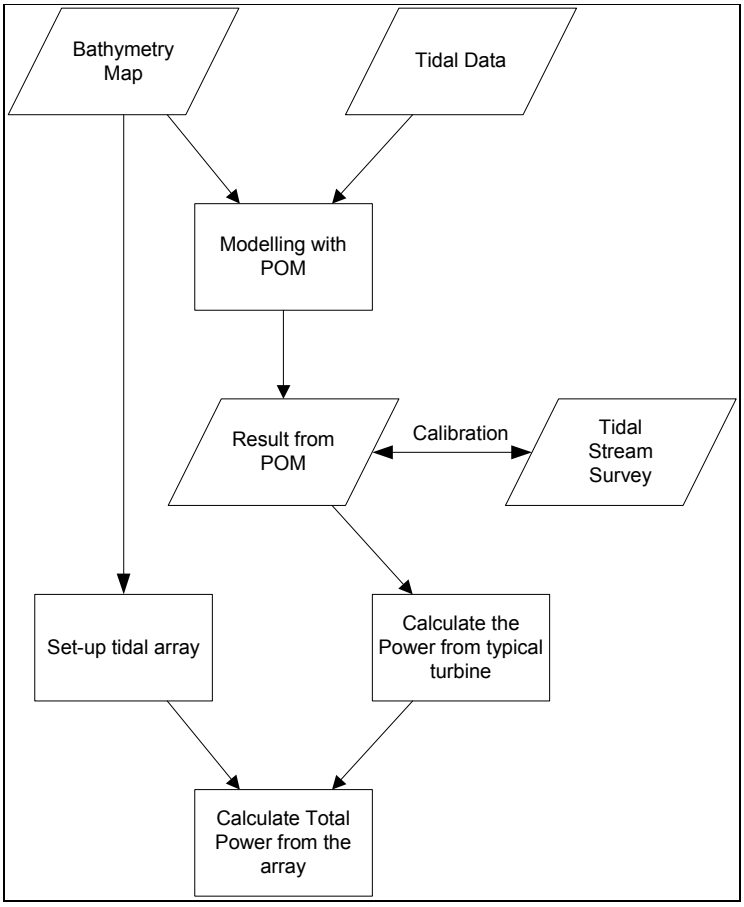

Figure 4.3: Alas Strait tidal energy resources assessment flowchart.

The step by step methods are:

1. Collecting data. The data needed for this project are explained in previous section.
2. Converting raw data to POM-based input data. The bathymetry map needs to be scanned first. The scanned version file format is DWG (AutoCad-type file). This file is then converted to initial condition data for POM using Matlab function. The format of the tidal data needs to be arranged to suit POM format.
3. Modelling with POM. Ensure the prescribed components constant is correct and represent the real conditions in Alas Strait. These components are:
    a. Internal and external time step
    b. Duration of program running
    c. Bottom roughness
    d. Bottom friction coefficient
    e. Smagorinsky diffusivity coefficient

f. Prandtl number
g. Background viscosity
h. Number of logarithmic layers at the surface and bottom
i. Jerlov water type

Other than those components, the boundary condition is defined according clamped elevation from the tide data.

4. Calibrating the results from POM to the data from tidal stream survey. If the results can not be confirmed to the data, the model needs to be corrected until the results show similarity with the data.
5. Calculating the power that can be generated by typical turbine using equation 2-8. However, the power can be generated only at times when the velocity is higher than the cut-in velocity.
6. Setup tidal array. The methods to setup the tidal array are:
    a. Identify critical depth and avoid shallow area
    b. Select MCT diameter with consideration of equation 2-9.
    c. Create sub-array with consideration of lateral and longitudinal spacing between MCT.
    d. Select downstream spacing of sub-array.
7. Calculating the total power from the array. This can be done by multiplying typical power of typical single turbine, blockage ratio, and number of turbines.

5 MODEL SETUP

The hydrodynamic model used in this project is the Princeton Ocean Model (POM). As mentioned in the earlier chapter, this model uses a Cartesian coordinate system in the horizontal and sigma coordinate for the vertical. The Alas Strait's elevation data in figure 5.1 below are created using sets of program in Matlab (see Appendix A3). These set of programs are intended to be used to convert CAD Data into utilizable text-based format (ASCII). The elevation data have 201 x 221 grid points which cover area from -9.2° to -8.1° N and from 116.3° to 117.3° E. Each of the grids has resolution of 0.005° x 0.005°.

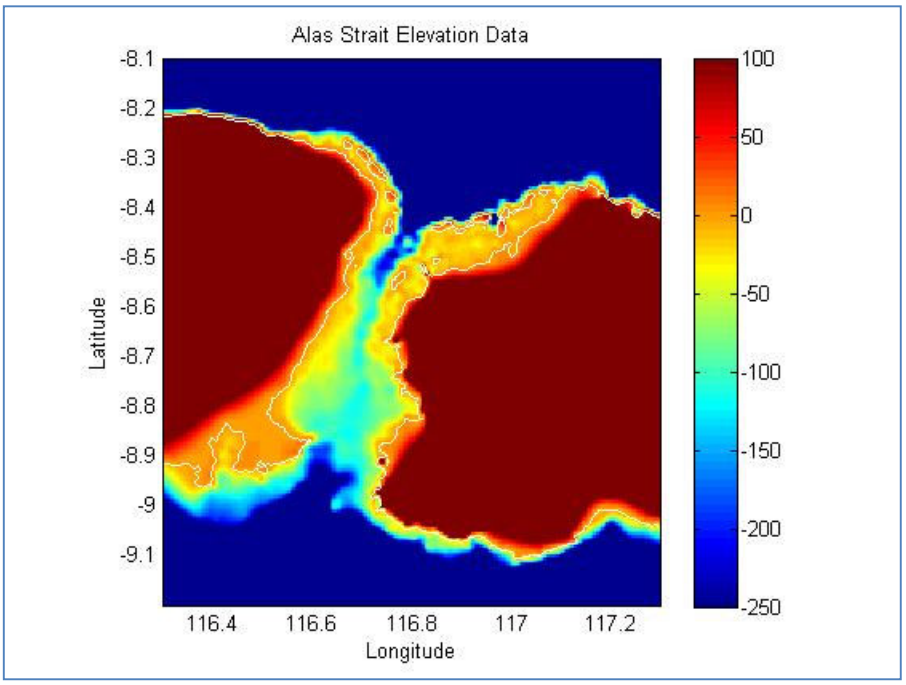

Figure 5.1: Alas Strait Elevation Data

5.1 Initial Condition

The Alas Strait's elevation data, which have ASCII format-data, are then used as an input in program Grid.f (see Appendix A4) to create the initial condition file. In this case, the original Grid.f file has been modified to accommodate the Alas Strait's condition.

The initial condition file for POM consists of bottom topography, initial wind velocity, initial condition of surface temperature, and also salinity. Since the wind velocity, temperature, and salinity are not significant for assessing tidal energy, the value of these parameters have been set to be constant for all locations. The wind velocity,

salinity, and surface temperature values used are zero, 35 psu, and 20° Celsius, respectively.

The initial condition model is created by defining the location of each end of the model domain as follow:

- The location of the south-west corner is 6.4° E and -9.15° N
- The location of the south-east corner is 7° E and -9.15°N
- The location of the north-west corner is 6.6° E and -8.15° N
- The location of the north-east corner is 7.2° E and -8.15° N.

This model uses curvilinear grid, and the grid number (i for horizontal and j for vertical) starts from the south-west corner (i=1, j=1) and ends at north-east corner (i=81, j=121). The model can be seen in figure 5.2 below. The land is represented by the white colour.

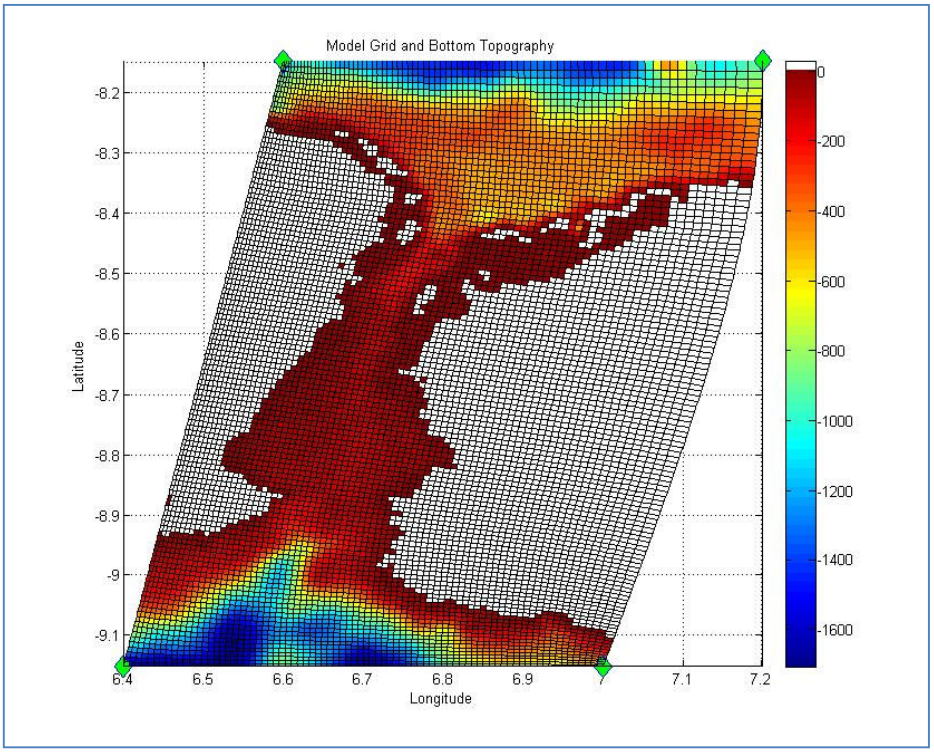

Figure 5.2: Alas Strait Model Grid and Bottom Topography

The horizontal domain of the model is divided into 81 x 121 grid points. The grid size is approximately varied between 800 to 850 meters in x-direction and 900 to 950 meters in y-direction. Note that x and y direction for this case is relative to the grid instead of to the longitude and latitude.

The vertical domain is divided into 25 unequal system levels (σ = 0 at sea surface and σ = -1 at sea bottom) with higher resolution on the bottom to resolve bottom boundary layer. The five sigma layers nearest to the bottom are σ = -0.9048, -0.9524, -0.9762, -0.9881, -0.9940, and -0.9970.

An example of the implementation of the sigma layer for the model can be seen in figure 5.3 below. This location of j=60 is located exactly in the middle of the channel. In the picture, it can be seen the representation of temperature distribution on different layers. It shows that temperature is exponentially decreased according to depth. Note that the figure is not presented in a balance range; the x-axis is in longitudinal degrees while the y-axis is in meters.

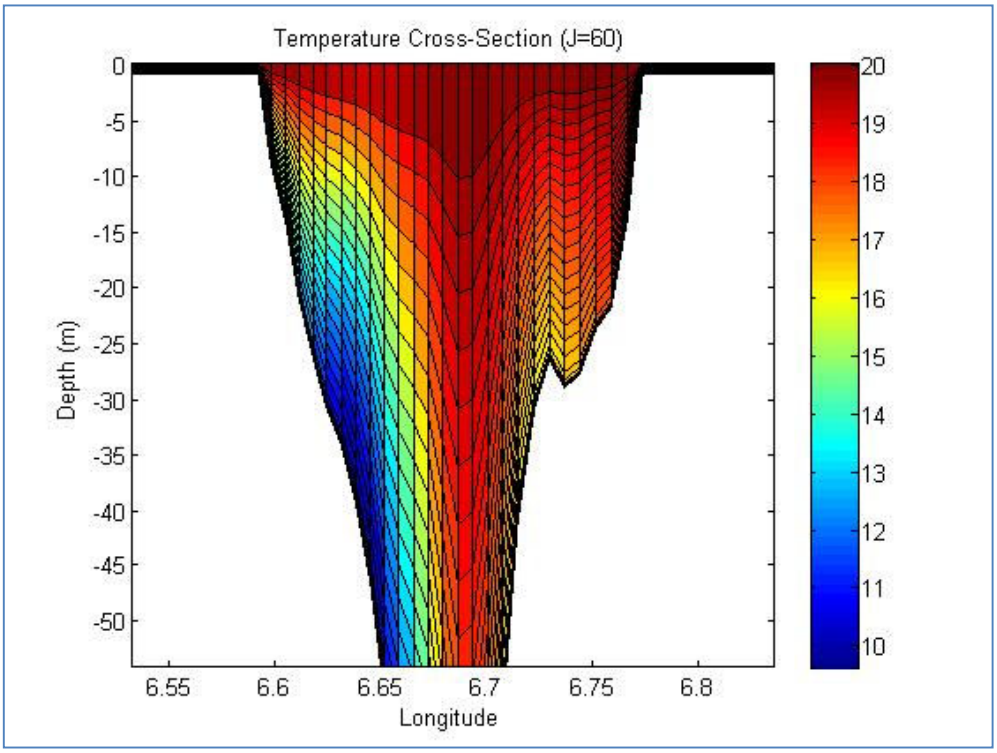

Figure 5.3: Temperature cross section at grid J=60 of Alas Strait Model.

The initial condition file is then used as an input file to create Alas Strait model using POM.

5.2 Prescribed Parameters

In this study, water density is assumed to be homogeneous with the value of 1025 kg/m^3. The vertical eddy viscosity is computed using the Mellor and Yamada (1982) level 2.5 turbulent closure scheme. The horizontal eddy viscosity is calculated using the

shear-dependent Smogorinsky formulation with coefficient 0.2. The inverse horizontal turbulent Prandtl number used is 0.2 and the Jerlov water type used is type 1a.

Note that the bottom-stress and friction velocity in the present sigma-coordinate model are calculated using the currents and the drag coefficient at the lowest current level, which is depth dependent. Bottom stress is obtained by quadratic drag law in which the drag coefficient is calculated on the basis of specified bottom roughness length, 0.01 m for this case.

The external time-step used to run the simulation is 1 second, while the internal time-step is 3 second. The simulation is run for 6 days with the starting time at 12 am of the 5 December 2007. The output is written in netcdf format with the time interval of 0.05 days.

The complete POM model for Alas Strait is presented in Appendix A5. It includes the modified POM08 program, the prescribed parameters (params), initial condition file (fort.40), and boundary condition file (bcond.f).

5.3 Boundary condition

The closed boundary (land mass) condition for Alas Strait model is defined by using mask. The mask sets the horizontal and vertical flux to the land boundary to be zero.

The open boundary conditions have critical impacts on a regional tidal model. Solutions in model interior are uniquely determined by the tidal open boundary conditions (Zhang et al., 2003). However this often becomes a problem since one of the most difficult problems in shallow water modelling is the uncertainty of the open boundary condition (Chu et al., 1997).

The open boundary for Alas Strait model uses clamped elevation. It defines the tidal elevation on the boundary for every time using equation 5-1. This equation is based on equation 2-42, but the value of equilibrium when t=0 (E) is defined as $Vtide_i + Utide_i$.

$$h_i(t) = \gamma_i A_i \cos(\varpi_i t + Vtide_i + Utide_i - \theta_i) \qquad (5\text{-}1)$$

Where i = index of the model grid along the open boundary

h = tidal elevation along the open boundary

γ_i = nodal correction for amplitude

A_i = tidal constituent amplitude

θ_i = epoch / tidal phase

ϖ_i = angular speed

$Vtide_i$ = nodal correction for phase 1

$Utide_i$ = nodal correction for phase 2

t = time

There are eight tidal constituents used, including: M_2, S_2, N_2, K_2, K_1, O_1, P_1, and Q_1. The value of tidal amplitude (A), tidal phase (θ_i), and angular speed (ϖ) for each constituents are obtained using OTIS from "Indonesian Seas Inverse Tidal Solution". The complete input and output of the OTIS model used in Alas Strait Model are shown in Appendix A-6.

The nodal corrections for amplitude and nodal correction for phase are calculated in Appendix A-7. For this calculation, the date is set at the beginning of the model running, which is on 5th December 2007. The summary of the calculation for each tidal constituent can be seen in table 5.1 below.

Table 5.1: Nodal correction for 8 tidal constituents at 5 December 2007

No.	Tidal Constituents	γ	$Vtide$ (degrees)	$Utide$ (radians)
1	M_2	0.6373087	75.46324	-0.386119
2	S_2	1	0	0
3	N_2	0.6373087	264.28176	-0.386119
4	K_2	1.3149362	149.80307	-2.995704
5	K_1	1.1279298	164.90154	-1.393492
6	O_1	1.2080492	90.561705	1.5714024
7	P_1	1	15.098465	0
8	Q_1	1	279.38022	0

The example of surface water elevation for the northern boundary condition for six days can be seen in figure 5.4 below. The location is the south-west end of the model

(i=1, j=1). Figure 5.5 shows the elevation boundary at the north east end of the model (i=81, j=121).

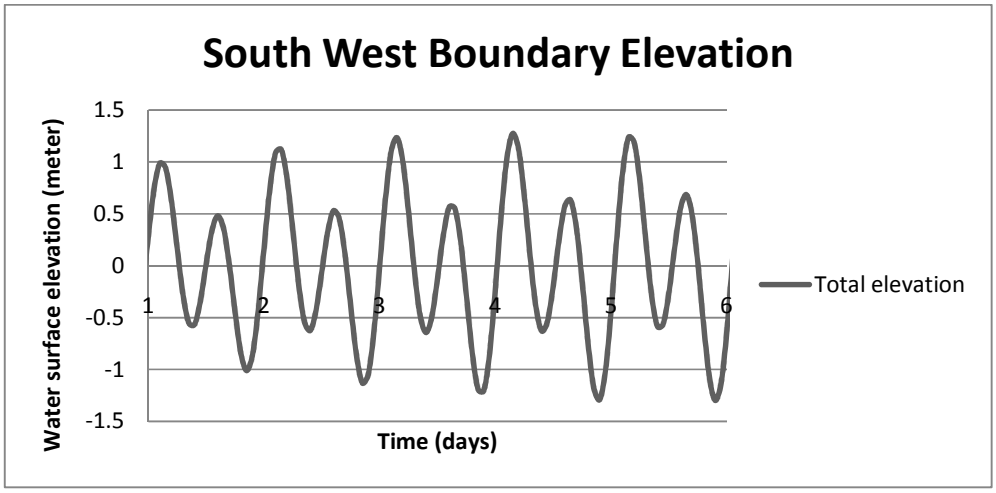

Figure 5.4: Elevation boundary condition at south west end location (i=1, j=1)

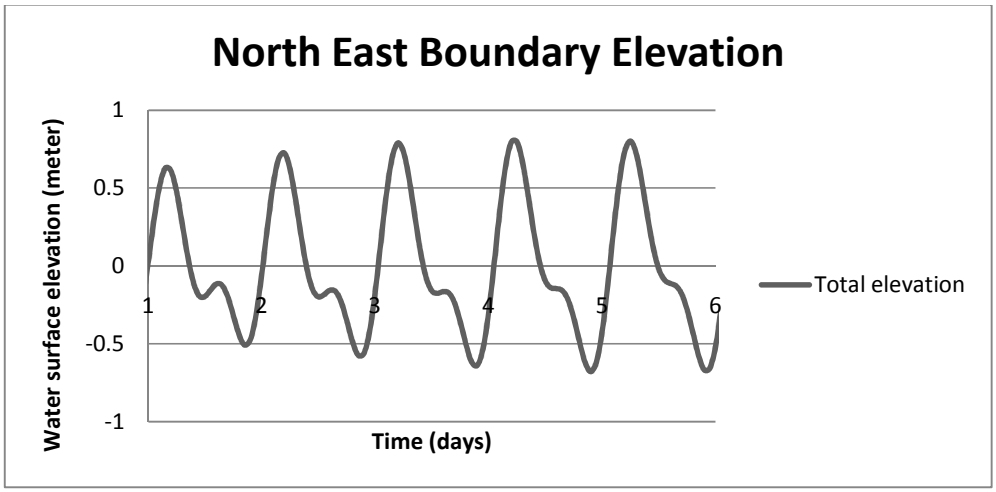

Figure 5.5: Elevation boundary condition at north east end location (i=81, j=121)

However, on the Alas Strait POM model, ramp is applied for the first day to prevent the velocity blow-up on the model. The ramp is set as the time for time less or equal to one day, and set as 1 for time more than one day. The boundary condition is defined in subroutine bcond.f (see appendix A5).

5.4 Model Validation

According to Blunden & Bahaj (2006), validation of the model can be done using comparison of the model with the actual condition. The comparisons that can be used are:

- Tidal elevation comparison
- Tidal diamond comparison
- Flow speed comparison

For Alas Strait model, the flow speed becomes the validation data. This is due to the fact that the only measurement data available for Alas Strait is the current velocity. The location of the survey is shown in figure 4.2. This location is equal to grid i=27, j=73 on the model.

Since during the first day, ramp is implemented to the model to prevent data transient; the comparison between the model and the data is started at the second day (6th December 2007). The comparison can be seen in figure 5.6.

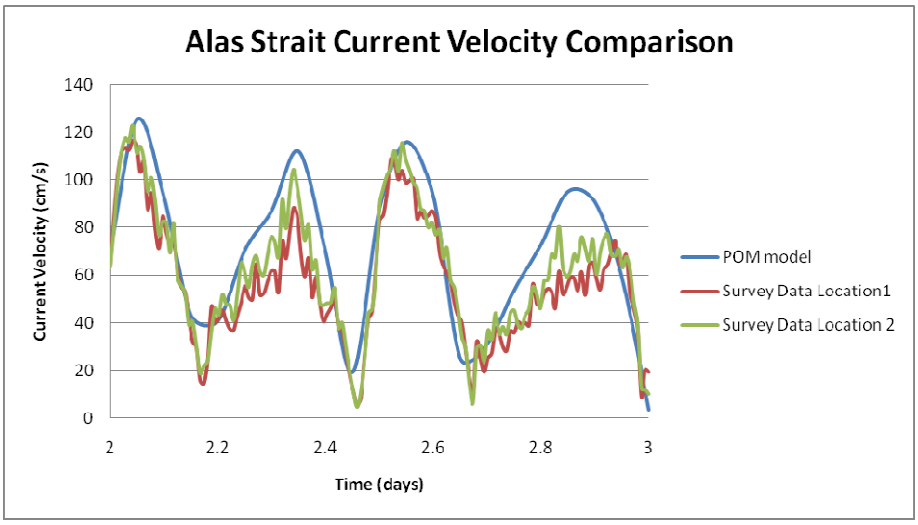

Figure 5.6: Alas Strait current velocity comparison in survey location (i=27, j=73)

Note that on the figure above, the current velocity of the model is the total current velocity in centimetres per second, neglecting the direction. The total current velocity is calculated using equation 5-2 below:

$$U_{tot} = \sqrt{U^2 + V^2} \qquad (5\text{-}2)$$

Where U_{tot} = total current velocity

U = depth average current velocity in x-direction

V = depth average current velocity in y-direction

Based on the figure 5.6, it is shown that even though the model's results and the data are not exactly similar, both are showing the same trend. In addition, it shows that the strongest current velocity shows the same magnitude. It is also important to notice that the comparison with current velocity is typically less accurate than the surface elevation comparison, thus makes the figure 5.6 above relatively good. The figure only compares the third day of the simulation, start at 12 am 7th December 2007 to 12 am 8th December 2007.

The difference between the data and the model could also occur due to the fact that current velocity can also be created by wind and wave. This could introduce noise to the measurement data. Therefore, it can be concluded that the model is validated by the survey data.

6 POWER FROM TYPICAL SINGLE TURBINE

6.1 Typical Turbine Specification

The typical marine current turbine used for this assessment is based on a model of the Seagen. The illustration of the Seagen design can be seen in figure 2.3, while the illustration of its implementation in array can be seen in figure 6.1 below.

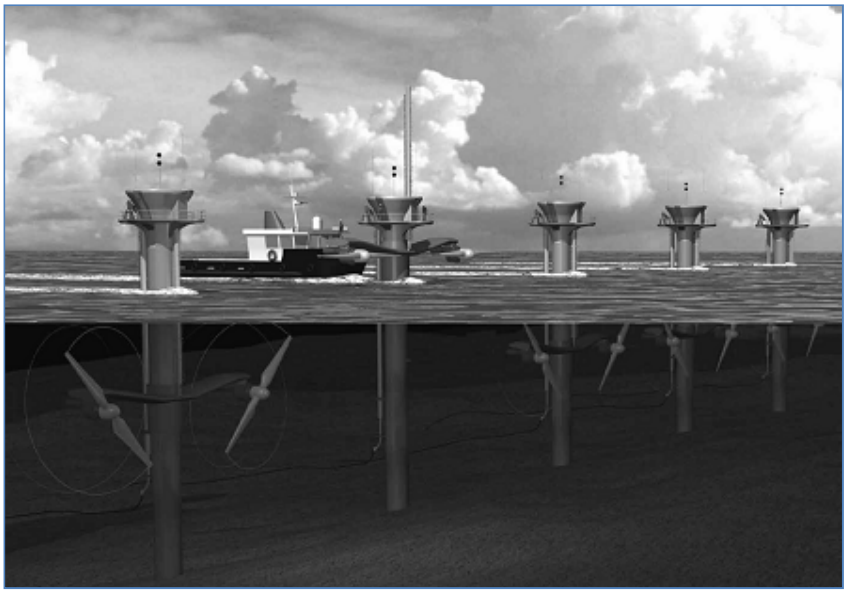

Figure 6.1. Artist's impression of Seagen turbines array. Source: Fraenkel, 2007.

This turbine system has rotors mounted at the outer ends of a pair of arms projecting on both sides of the supporting pile. The diameter of each rotor is expected to be in the range of 14 m to 25 m. The decision to neglect diameter smaller than 14 m is based on the cost-effective ratio, i.e. the cost of implementing turbine with diameter less than 14 m is higher than its electricity generation. A rotor with diameter more than 25 needs a high lift force which caused by a high mass flow and a low velocity of the water particle. This could result in bending of the rotor blades, especially for a rotor with a bigger diameter blade.

The design of twin rotor turbine allows the turbine to generate energy twice of that generated by a single turbine, so it enhances the cost-effectiveness. Another reason for the twin rotor configuration is that this permits bidirectional operation with the rotors clear of the pile wake when the rotors are downstream of the pile; 180° rotor blade pitch control allows efficient operation when the current reverses (Fraenkel, 2007).

The main support structure is a steel monopole with diameter around 3 m. The 'cross arm' structure which used to hold the rotor is elliptical and is designed to minimise the wake thickness. The power system is expected to be similar with Seagen which used variable speed, variable voltage, and variable frequency. These variables are controlled by control system to vary both the frequency converter's parameters and the rotor blade pitch angles in order to optimise its performance.

6.1.1 Cut in speed and power rated

The system is designed to reach a successful start-up by initiating rotation without generation. The rotations will start the generation process at a cut in speed. The cut-in speed is the minimum current velocities that start the turbine rotation's initiation. The system then seeks to maximise the power until the current speed reaches a level where the rated power is achieved, which is typically set at around 70% of the mean spring maximum tide velocity depending on the local site conditions (Environmental Change Institute, 2005).

The original Seagen has cut-in speed of 0.7 m/s and rated power at 2-2.3 m/s (Fraenkel, 2007). By using analogy that rated cut in-speed is set as a percentage of the rated power, it is found that the cut-in speed is set at 30-35% of the rated power. Applying the same analogy for Alas Strait, maximum spring current velocity in Alas Strait is around 1.85 m/s (from site measurement), this makes the rated power to be at 1.3 m/s and the cut-in speed at 0.4 m/s.

For current velocities at above the rated power, the power is shed using the pitch-control mechanism by reducing the angle of attack of the blades to maintain as close to rated power as possible. When the system reaches the cut-in speed again, the system cuts out and the rotor is stay still. When the direction of the flows changes, the control system will pitches the rotor blades to the direction of upcoming flow. This procedure then takes place continuously.

6.1.2 Rotor diameter

The typical rotor diameter's sizes for this assessment are based on Myers & Bahaj (2005). The diameter (size) of the rotor, nominal operating depth, and its hub height are summarised in table 6.1.

Table 6.1. Typical rotor diameter parameters

Rotor diameter (m)	Nominal operating depth (m)	Hub height above seabed (m)
14	28	14
20	36	19
25	40	20.5

Based on previous studies (as mentioned in section 2.3.3), it is assumed for Alas Strait case that the power coefficient (C_P) of 0.35 at rated speed is used.

6.2 Method

The power from typical single turbine is calculated using the following steps:

1. Extract the the current velocity from the selected grid
2. Calculate the total current velocity for each time using equation 5-2.
3. Calculate the power using equation 2-8. The typical turbine parameter (for all rotor diameter) in section 6.1 is used as input.
4. Perform this calculation for five days from second day onwards.
5. Calculate the average power per day, average power per month, and average power per year.

6.3 Result

The result presented in this section is only an example using tidal stream data from Alas Strait model in survey location (i=27, j=73). The 5 days comparison of power that can be generated by typical turbines is shown in figure 6-2 below.

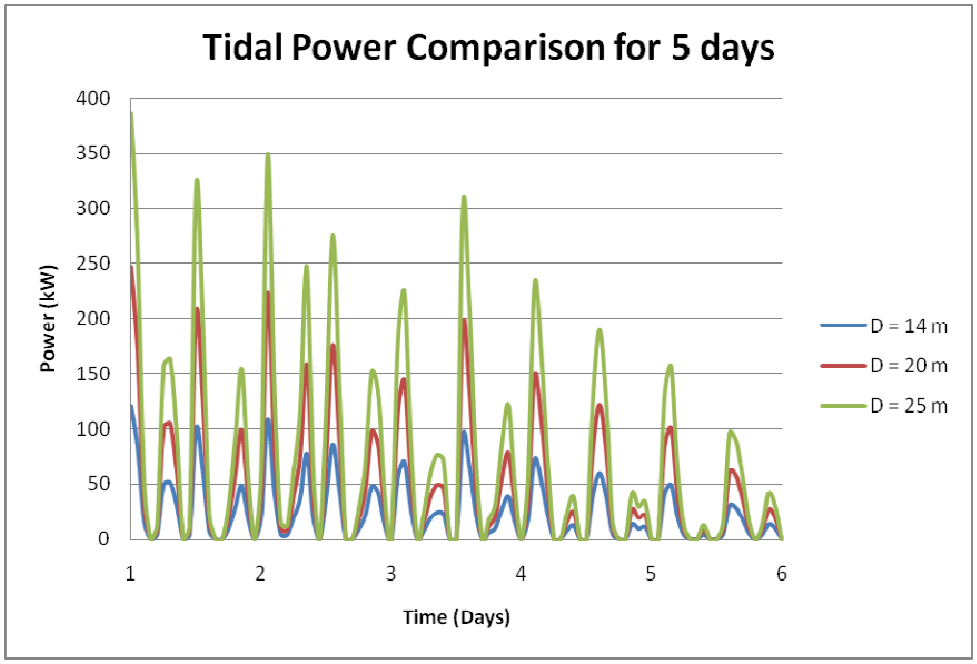

Figure 6.2: Five days tidal power comparison of three typical diameter turbines in survey location

For a clearer interpretation, the comparison of tidal power that can be generated is shown in a shorter time period (24 hours). This can be seen in figure 6.3 below.

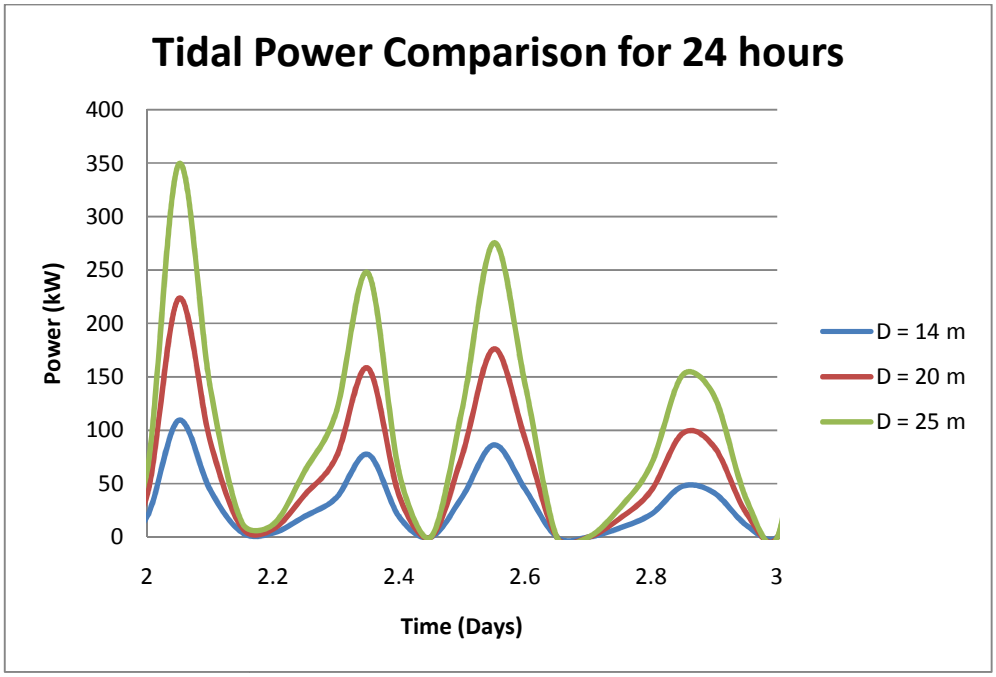

Figure 6.3: 24 hours tidal power comparison of three typical diameter turbines in survey location.

The summary of typical turbines power is presented in table 6.2. Note that the average power per day is calculated by dividing the total power in 5 days with the number of days, i.e. 5. The average power per month is calculated for 30 days by multiplying the average power per day with 30, while average power per year is calculated for 365 days.

Table 6.2. Summary of the typical turbine power in survey location

Rotor diameter (m)	**14**	**20**	**25**
Rated power (kW)	121.33	247.61	386.9
Total Power in 5 days (kWh)	1968.038	4016.403	6275.63
Average Power per day (kWh)	393.6075	803.2806	1255.126
Average Power per month (MWh)	11.808	24.098	37.654
Average Power per year (MWh)	143.667	293.197	458.121

Equation 6-1 is then used to calculate the effectiveness of the turbine. Capacity factor is the percentage of power generated by the turbine compare relative if it generated by constant rated velocity (full power). The rated power of each typical turbine for 5 days is calculated using the constant rated velocity of 1.3 m/s. This results in capacity factor of 13.5% for the typical turbine.

$$CF = \frac{\bar{P}}{\bar{P}_{rated}} \tag{6-1}$$

Where CF = Capacity factor

$\bar{P}$ = Power from the turbine

$\bar{P}_{rated}$ = Rated power from the turbine

6.4 Discussion

As mentioned before, the average power output from the turbine is calculated based on the average from five days modelling result. This method is implemented to save modelling and calculation time for the project. This method has weakness in lesser accuracy compared to the conventional method.

Considering the fact that the Alas Strait model is run in between the spring tide and neap tide, it captures the middle between the highest and the lowest current velocity.

These conditions happen most of the time, and consequently the average condition is expected to occur during this time. With the running time of five days, it expects that the average of it gives a solid representation to the whole tidal condition in Alas Strait.

This method also has the advantage in computation time as compared to the traditional method using 30 days modelling. This method is likely highly suitable to be used in a preliminary study, where quick result with good approximation of the whole area is needed.

Based on the low capacity factor, 13.5%, rated power might be too high for economic generation. This means that lower rated power is required. Thus, smaller rated velocity is more suitable for the site.

For further research, the comparison of the result between this method and conventional method is needed. Longer time-series will result in better constrains in power estimation. Other than the above, method worth mentioning is the method used by Pangastuti (2005) in which the average current velocity between spring tide and neap tide is used to calculate the average power per day.

The rated power in Alas Strait is considerably low as compared to some sites in the UK (Alderney Race for example). This is expected since the tidal current velocity in Alas Strait is relatively low (less than 2 m/s most of the time).

7 TOTAL POWER FROM THE TIDAL ARRAY

The total extractable tidal power from the Alas Strait is calculated based on the farm method using two scenarios. The first scenario uses the contemporary limiting water depth for Marine Current Turbine (MCT) installation. In this scenario, the tidal array is only installed in depth equal or less than 40 meter. This scenario is based on the current state of technology of MCT which still only permitted bottom foundation based MCT.

The second scenario applies the assumption that the depth limitation of MCT will get overcome in the future with the introduction of floating based MCT structures. This condition permits MCT to be installed in a deeper water depth. However, the limit of water depth is still required considering the need for anchoring the floating MCT structure and connection to the grid. For this case, the maximum water depth of 80 meter is used.

7.1 Tidal array configuration

Considering all factors for configuring tidal array as described in 2.3.4, the MCT array consists of multi sub-arrays. Each sub-array will consist of two rows of MCT. The number of sub-arrays per row is varied from each typical rotor diameter. For this assessment, to make the calculation more accurate, the size of a grid in the model is set as limiting size of sub-array. This makes each sub-array to be assigned into a specific grid, using its grid current velocity for the calculation.

The lateral spacing between MCT is set as three times the diameter. The width of each sub-array is set to be in the range 700-750 meter. The space different between the grid width and tidal array width is used to accommodate the minimum lateral spacing between sub-array of 200 meter (Myers & Bahaj, 2005).

Furthermore, using the same principle as Myers and Bahaj (2005), longitudinal spacing between rows in sub-array is set to be fifteen times the diameter. There is also a requirement to keep the minimum longitudinal spacing between sub-arrays to be 500 m. The minimum spacing between sub-array – both longitudinal and lateral spacing – is also intended to allow access for maintenance craft.

The parameters of each typical sub-array based on MCT rotor diameter is shown in table 7.1 below.

Table 7.1. Parameters of the sub-arrays based on MCT rotor diameter

Rotor Diameter (m)	Lateral spacing between MCT (m)	Sub-Array		
		Number of Turbine per row	Width (m)	Longitudinal spacing between row (m)
14	42	14	742	210
20	60	10	740	300
25	75	8	725	375

7.2 Method to calculate power from tidal array

The method to assess the tidal array layout and power in Alas Strait is based on the method used by Myers and Bahaj (2005) with some modification applied. Other than the typical sub-array dimension as mentioned in 7.1, another major difference is the use of current velocity according to the grid, instead of using one typical current speed for the whole area.

The downstream current speed decay is implemented to the calculation. The value of the downstream current velocity is calculated using equation 2-10 with rotor axial induction factor of 0.25. This results in the value of row velocity decay factor (R_{DF}) as: (1) 0.894 for downstream of sub-array with 14 m rotor, (2) 0.882 for downstream of sub-array with 20 m rotor, (3) 0.867 for downstream of sub-array with 25 m rotor (Myers & Bahaj, 2005).

However, the latest study on the wind speed deficit loss in offshore turbine arrays (Frandsen et al., 2006), shows that after the fourth row, there is no significant decrease of the wind speed. This phenomenon occurs due to the merging of multiple winds wakes after turbine row. Therefore for Alas Strait assessment, it is assumed, based on the similarity of offshore wind turbine array with MCT array, that there is no current velocity loss after the fourth row (or second MCT sub-array for this case).

The illustration of the method used in calculating downstream velocity is shown in figure 7.1.

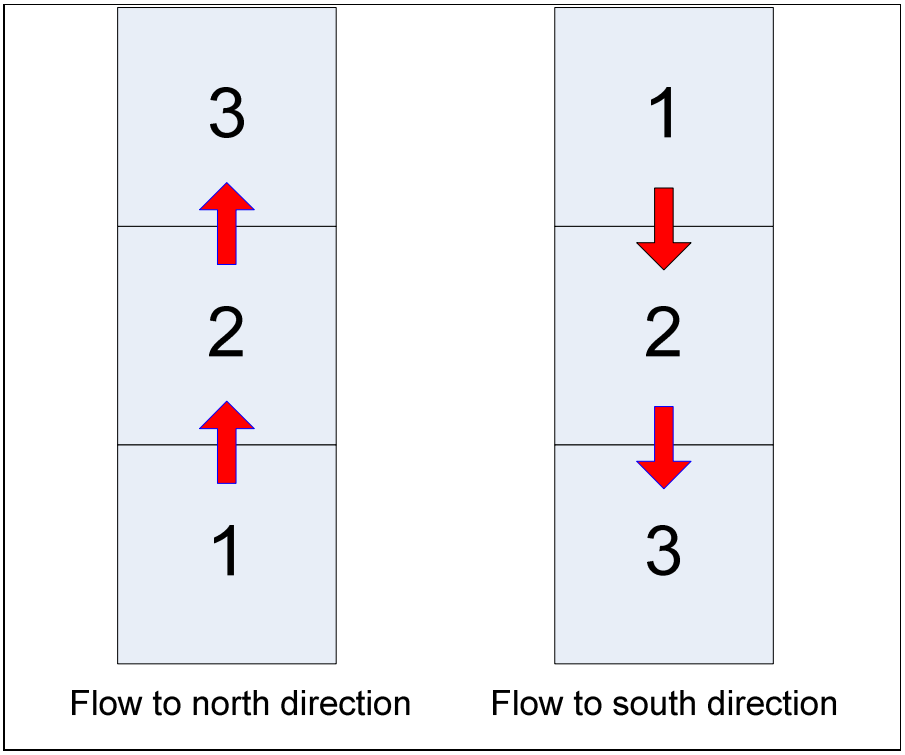

Figure 7.1: Illustration of the method to calculate the downstream flow velocity

Using the three grid example from figure 7.1, if the flow goes to the north direction, the southernmost sub-array becomes the first row with the northernmost sub-array becomes the third row, while if the flow goes to the south direction, the northernmost array becomes the first row and the southernmost grid becomes the last row. It means that the value of row velocity decay factor (R_{DF}) of the second row will be influenced by the downstream of the first row, depending on which grid-array becomes the first row.

The method to calculate the annual tidal array power is summarised with following steps:

1. Based on the site bathymetry, identify the critical depth and avoid shallow area.
2. Select typical sub arrays suitable for the grid area (based on the depth).
3. Based on the current velocity from model result, select the initial site location. Use only grid with velocity higher than 1.2 m/s.
4. Use only grid with connection to another grid that suitable based on the above criteria. So, there is no distance between grids chosen as sub-array.
5. Calculate the R_{DF} for each sub-array.
6. Calculate the current velocity downstream.

7. Calculate the power of the tidal sub-array by multiplying power from single turbine (similar with calculation in chapter 6) with the number of turbine in the sub-array.
8. Calculate the total power of the array by adding up power from all sub-arrays.

7.3 Total energy with depth limitation scenario

The grid that suitable to be assigned as sub-array is shown with yellow, green, and light blue colour in figure 7.2 below. The red colour indicates shallow depths (less than 24 m), the yellow colour represents sites suitable for typical 14 m MCT diameter, whilst the green colour indicates sites suitable for typical 20 m MCT diameter. The light blue indicates sites suitable for 25 m MCT diameter.

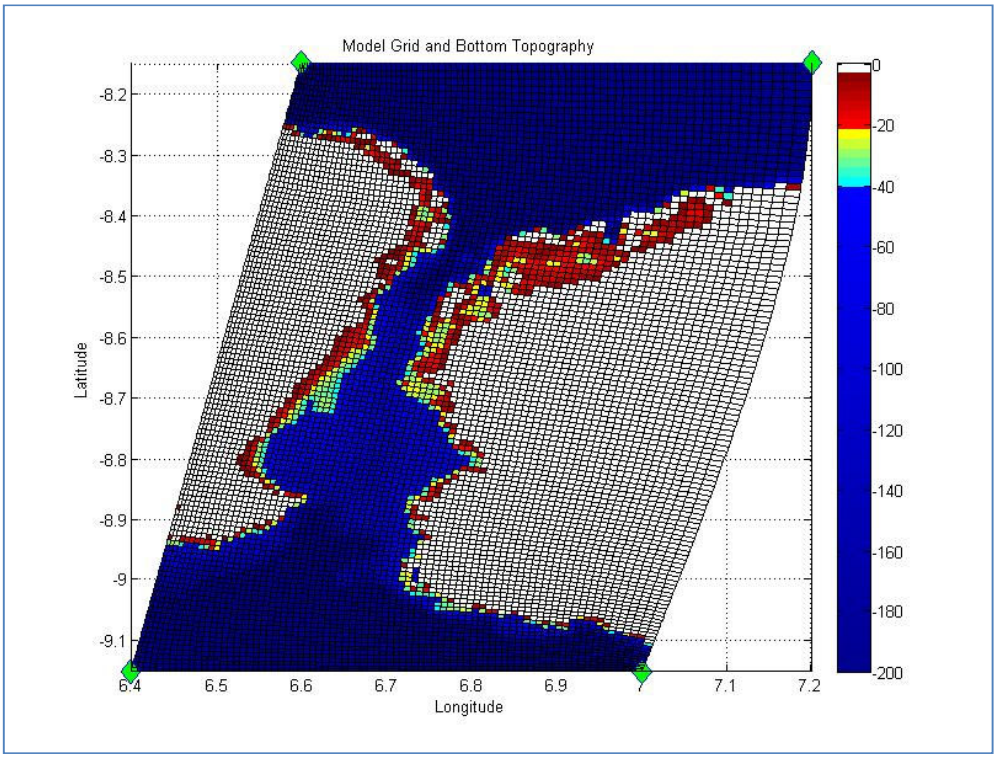

Figure 7.2: Acceptable location of tidal array according to the depth for depth limitation scenario.

After considering the current velocity of the above grid, the tidal array configuration for depth limitation scenario is selcted. Figure 7.3 shows the tidal array configuration. The number assigned to array is the indicator of the MCT sub-array dimension for each particular grid. The “14” indicates a typical MCT diameter of 14 m, “20” represents a typical MCT diameter of 20 meter, while “25” shows a typical MCT diameter of 25

meter. All sub-arrays are located at the west side of Alas Strait, since the nearest electricity grid is located near to the location.

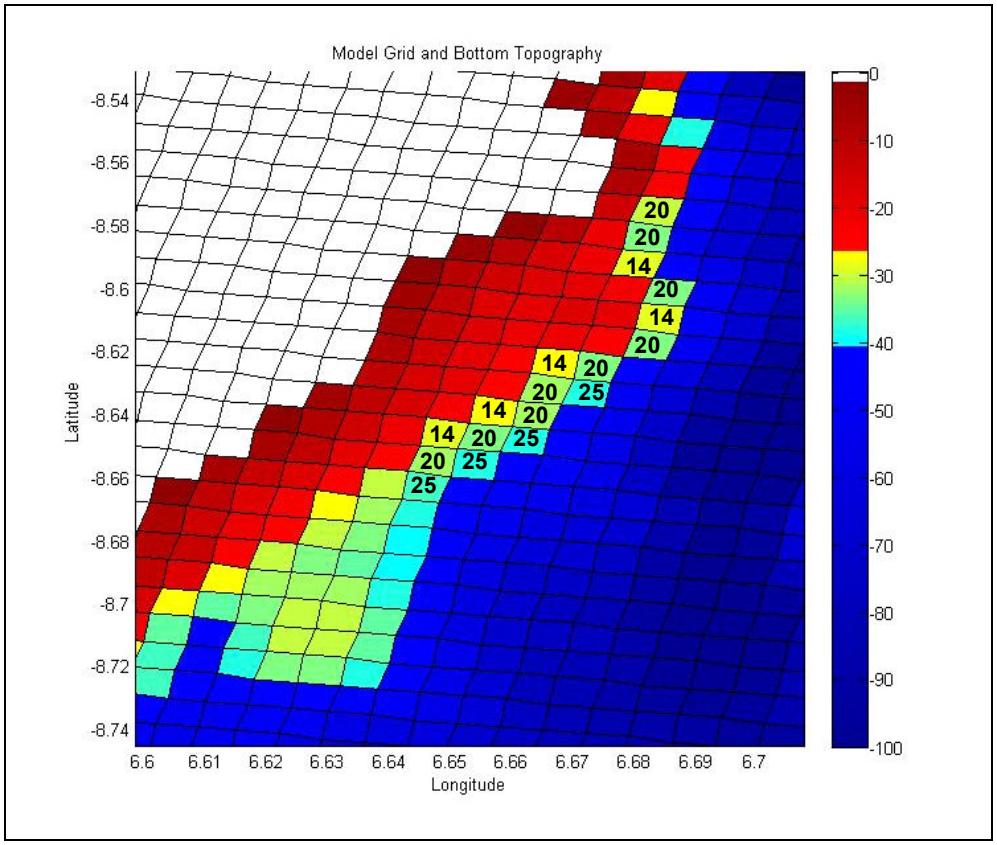

Figure 7.3: Tidal array configuration for depth limitation scenario.

The power from the array for 5 days and 24 hours for the depth limitation scenario is shown in figure 7.4 and 7.5 below.

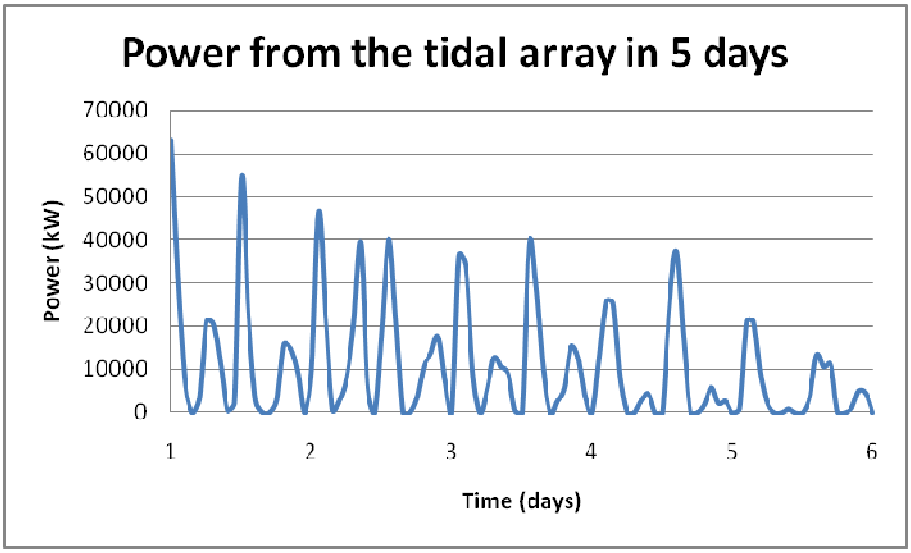

Figure 7.4: Power from tidal array in 5 days based on depth limitation scenario

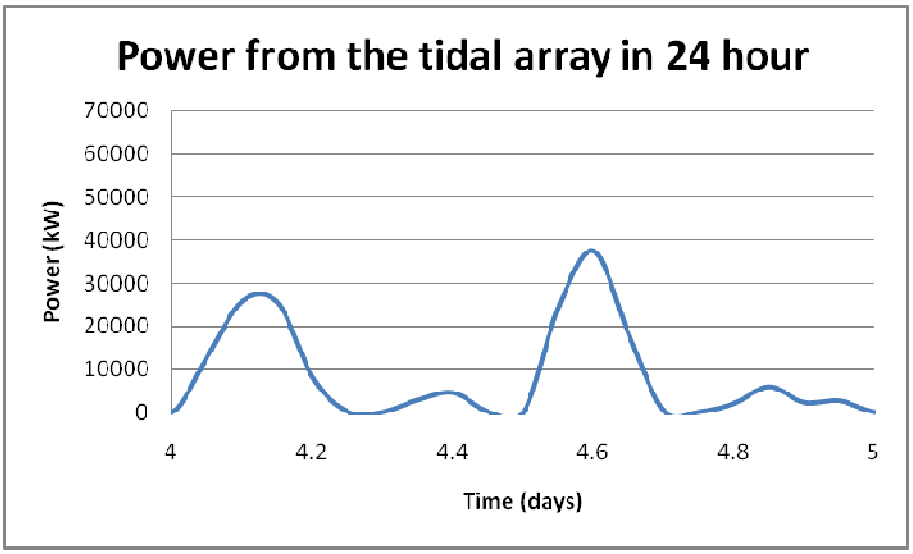

Figure 7.5: Power from tidal array in 24 hours based on depth limitation scenario

7.4 Total energy with application of floating MCT scenario

Using the same method as previous section, the suitable location for floating MCT scenario based on the depth is shown in figure 7.6 (shown by grids with yellow, green, and light blue colour).

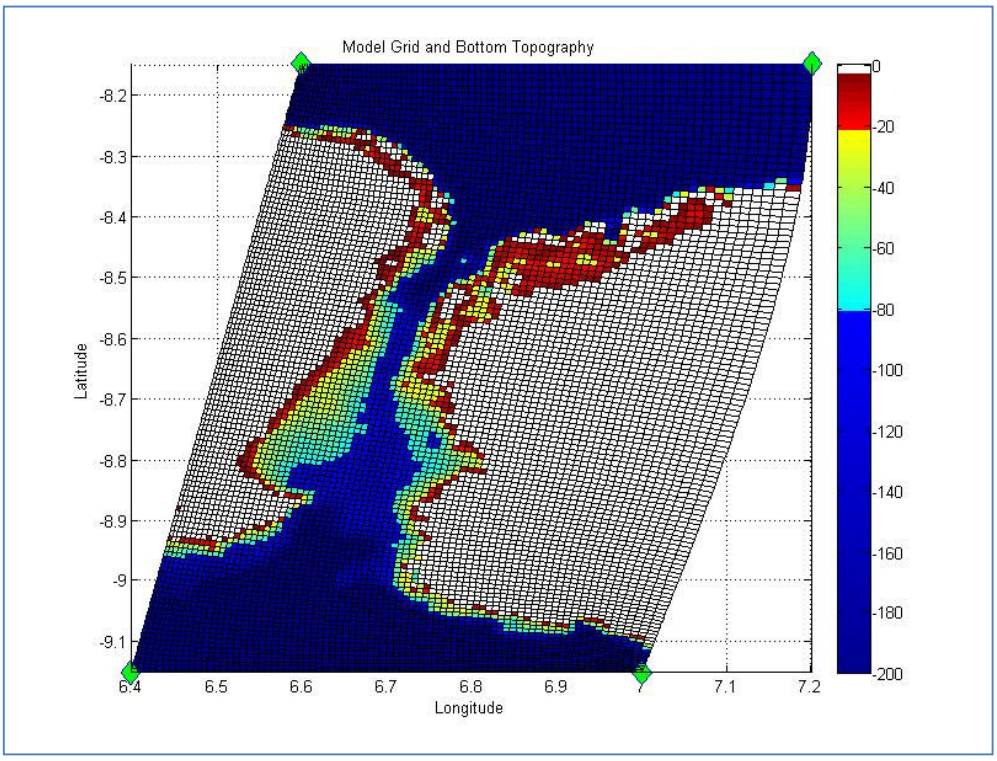

Figure 7.6: Acceptable location of tidal array according to the floating MCT scenario.

After considering the current velocity of the above grid, the tidal array configuration for floating MCT is chosen. Figure 7.7 below shows the tidal array configuration. The number assigned to array is the indicator of the MCT sub-array dimension for each particular grid. The “14” indicates a typical MCT diameter of 14 m, “20” represents a typical MCT diameter of 20 meter, while “25” shows a typical MCT diameter of 25 meter. Same as the depth limitation scenario, all sub-arrays are located at the west side of Alas Strait, since the nearest electricity grid is located near to the location. For site with depth more than 40 meter, the typical MCT assigned is the 25 meter diameter.

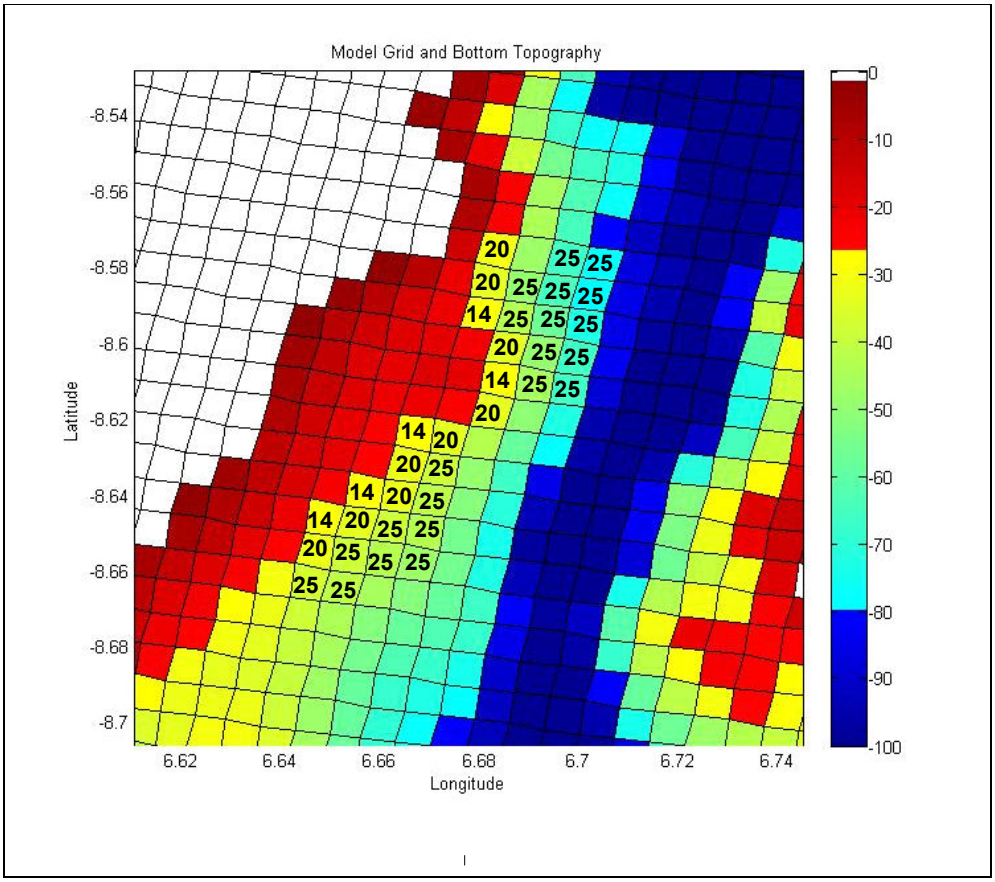

Figure 7.7: Tidal array configuration for floating MCT scenario.

The power from the array for 5 days and 24 hours for the depth limitation scenario is shown in figure 7.8 and 7.9 below.

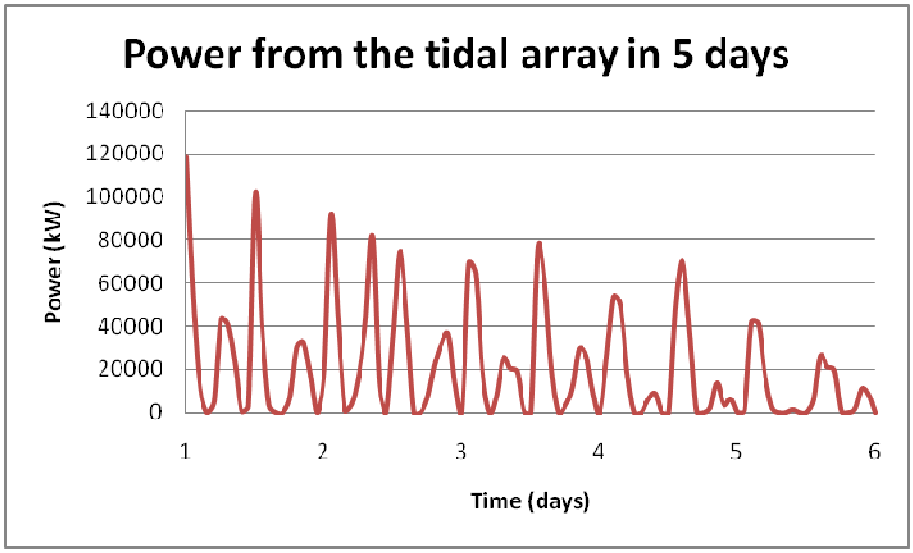

Figure 7.8: Power from tidal array in 5 days based on floating MCT scenario

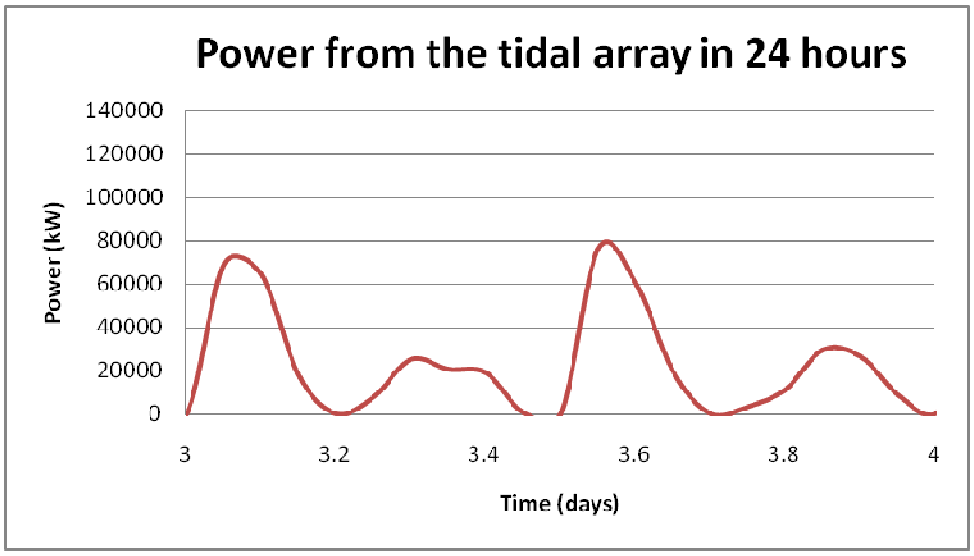

Figure 7.9: Power from tidal array in 24 hours based on depth limitation scenario

7.5 Discussion

To summarise the above calculation, table 7.2 shows the total tidal array power based on both scenarios. It shows that there is a considerably improvement of total power from the depth limitation scenario to floating MCT scenario. The floating MCT scenario also opens new possibilities in tidal energy development. However, this scenario is still

imaginary and unfortunately, it is still impossible to realise to this day due to the limitation of the technology. The implementation of floating MCT is expected in the near future, provided more attention to renewable energy is given with numbers of research and study.

Table 7.2. Total power comparison between depth limited scenario and floating MCT scenario

Scenario	Depth limited	Floating MCT
Total Power in 5 days (MWh)	902.189	1757.869
Average Power per day (MWh)	180.437	351.573
Average Power per month (GWh)	27.065	52.736
Average Power per year (GWh)	329.299	641.622

The new method for calculating downstream velocity is logically showing a better accuracy compared to the previous method. However, since it is based on study of the offshore wind turbine array, i.e.not necessarily for tidal array, the relation could be different. Therefore study about downstream current velocity in tidal array is needed.

Other than observations and theory, process studies which utilise regional numerical simulations have been employed to quantify the tidal energy flux (Lee et al., 2006) and dissipation (Klymak et al., 2006).

In their report, Blunden and Bahaj (2006) conclude that numerical model with validation; good resolution and sufficient amount of running time can predict the variation of tidal stream in time and space with confidence.

An important limitation in this study is that the POM model in Alas Strait is only validated using one location. To make the model accurate, typical measurement data from at least three locations are needed for calibration. However, as mentioned before, the availability of the data is often the problem in Indonesia.

This situation makes plenty of possibilities of error and uncertainties in the model. Other than an error comes from the different between actual condition and the model, uncertainties and error for this case could also be found in numerical model error. This error could be overcome by using smaller grid size with the expense of computation time. The reason for avoiding this for Alas Strait Model is since some modifications of the POM is needed in order to use smaller grid size in POM. The modifications require

re-writing some subroutines and need plenty of time. Other possible errors include the iteration error which arises when the iterative process is incomplete and round-off error that depends on the digit of accuracy of POM.

On top of the above errors, the error could also caused by user error. Note that the term “error” means recognisable deficiency which the cause is not due to lack of knowledge, while “uncertainty” means potential deficiency due to lack of knowledge.

8 CONCLUSIONS

After conducting this study, the main conclusions drawn are summarised in the following:

1. Although there are many potential sites, only limited data are available (e.g. water elevation and current velocity). A complete and comprehensive data are needed to conduct a proper tidal energy resource assessment in Indonesia.
2. It has been shown that Princeton Ocean Model (POM) is able to simulate the flow conditions in Alas Strait. Even though the resolution of the model is still relatively low (more than 500 m grid size), its result shows a good result with calibration data.
3. Tidal current velocity in Alas Strait could reach up to 2 meter per second in a certain location during spring tide. Although this is not considerably high for tidal energy extraction, Alas Strait can be considered as a promising site for the implementation of tidal energy.
4. The new method of calculating downstream velocity of tidal array based on relative flow direction to the grid is shown to be effective to be used in tidal energy resources assessment.
5. When tidal array with current depth limitation ranging from 24 to 40 meter is used, the total annual tidal energy that can be extracted is 329.299 GWh.
6. When tidal array with future depth limitation (floating MCT scenario) ranging from 24 to 80 meter is used, the total annual tidal energy that can be extracted is 641.622 GWh.
7. It also shows that the tidal power that can be generated in Alas Strait is comparably lower than that in some of UK site such as Alderney Race. However, with plenty of prospective sites still remain to be assessed; Indonesia still has the potentials to implement the tidal energy.

9 RECOMMENDATIONS

From this study, an enhanced understanding has been gained in the energy resources assessment in Indonesia, especially in Alas Strait. This study should be considered as a small step in renewable energy development in Indonesia, especially in tidal energy frame. Some recommendations for further research are formulated below.

Ocean Model

In conducting a proper tidal energy assessment, modelling the actual condition as accurate as possible is needed. Princeton Ocean Model (POM) is able to model it and the result is considered as relatively accurate for this case. However, there are some limitations in it, such as: (1) the original program is better suited for regional scale model since the grid size cannot be smaller than 500 m, (2) the user has to re-write some part of the program to be well suited for specific locations, (3) the grid used is orthogonal and cannot be shaped according to terrain, i.e. it is not suitable for area with difficult geometry and shape. Therefore, it is suggested to use other programs that do not have similar limitations. Commercial 3D hydrodynamic simulation program such as Delft 3D, and RMA2 is more suitable in modelling sites with small size grid and complex geometry shape which results in a higher accuracy of the model.

Tidal energy assessment

One of the most important issues regarding tidal energy assessment is the spacing of Marine Current Turbine (MCT) and its influences to the downstream flow. Although some research has been conducted in this field of study, e.g. using bottom roughness coefficient to represent the MCT in the model, an accurate representation of the actual effect of the MCT to the flow is often overlooked.

Alas Strait

The model for this site cannot be categorised as an accurate model since it only has one location data to do calibration. Although the model result shows an agreement with the actual condition, it needs validation in other locations for the whole model to be called accurate. Therefore, more current velocity and surface elevation measurements need to be done especially in northern and southern part of the strait.

The boundary condition used for the model is clamped elevation condition, which proofed to be less accurate than using flather condition (see chapter 2). To used flather boundary condition, there is a need to define not just the water elevation but also the current velocity in the boundary. The development of a better regional tidal model could provide both data in the future.

The type of tidal energy device used to simulate the energy extraction in this study is based on the Seagen design. There are other types of tidal energy devices that might also be suitable for the location, such as Gorlov type turbine, and Stingray. Further study could be taken to do comparison between devices.

The configuration of the tidal array for this study is based on the configuration used by Myers & Bahaj (2005). Since tidal array configuration is site specific , further study could be conducted to find the most optimum tidal array configuration in Alas Strait.

Environmental impact of every project or new installation needs to be assessed. The effect of tidal energy extraction could harm the environment. The impact of the marine current turbine and its consequences on the flow and sediment transport is rarely investigated. Hence, EIA study in Alas Strait could become one of the first of its kind in South East Asia.

Indonesia

It is mentioned in chapter 3 that one of the major drawback in choosing site to be assessed in Indonesia is data availability. There are plenty of sites other than Alas Strait that worth to be assessed. However many of those sites are not suitable due to lack of data, especially data to calibrate the model result. Daily measurement of water elevation and current velocity are rarely to be carried out in Indonesia. If this problem could be overcome (i.e. if the data is available), sites that have potentials of tidal energy (e.g. Capalulu Strait in Maluku, Berau Bay in Papua, and area near Malacca Strait) can be assessed.

REFERENCES

Ainsworth, D. & Thake, J., 2006. *Final report on preliminary works associated with 1 MW tidal turbine*. DTI Technology Programme: New and Renewable Energy.

Bahaj, A. & Myers, L., 2003. Fundamentals Applicable to The Utilisation of Marine Current Turbines for Energy Production. *Renewable Energy*, 28, pp.2205-11.

Bahaj, A. & Myers, L., 2004. Analytical Estimates of Energy Yield Potential from the Alderney Eace (Channel Islands) using Marine Current Energy Converters. *Renewable Energy* , 29, pp.1931-45.

Bates, P.D., Lane, S.N. & Ferguson, R.I., 2005. *Computational Fluid Dynamics: Applications in Environmental Hydraulics*. West Sussex: John Wiley & Sons Ltd.

Batten, W., Bahaj, A., Molland, A. & Chaplin, J., 2006. Hydrodynamics of Marine Current Turbines. *Renewable Energy* , 31, pp.249-56.

Bennet, A., 1992. *Inverse method in physical oceanography*. Cambridge: Cambridge University Press.

Black & Veatch, 2005. *Phase II UK Tidal Stream Energy Resource Assessment*. London: The Carbon Trust.

Black & Veatch, 2005. *Tidal Stream Energy Resource and Technology Summary Report*. Middlesex: The Carbon Trust.

Blumberg, A. & Mellor, G.L., 1987. A description of a three-dimensional coastal ocean circulation model. *Coastal and Estuarine Science*, 4, pp.1-16.

Blunden, L. & Bahaj, A., 2006. Initial Evolution of Tidal Stream Energy Resources at Portland Bill, UK. *Renewable Energy* , 31, pp.121-32.

Blunden, L. & Bahaj, A., 2007. Tidal Energy Resource Assessment for Tidal Stream Generators. In *IMechE Vol.221 Part A: Power and Energy*., 2007.

Boruff, B., Emrich, C. & Cutter, S., 2005. Erosion hazard vulnerability of US coastal counties. *Journal of Costal Research*, pp.932-43.

Burton, T., Sharpe, D., Jenkins, N. & Bossangi, E., 2001. *Wind Energy Handbook*. New York: Wiley.

Carter, G.S. & Merrifield, M.A., 2007. Open boundary conditions for regional tidal simulations. *Ocean Modelling*, 18, pp.194-209.

Central Intelligence Agency, 2008. *The World Factbook*. Washington.

Charlier, R.H., 1982. *Tidal Energy*. New York: Van Norstrand Reinhold Company Inc.

Chu, P.C., Fan, C. & Ehret, L.L., 1997. Determination of open boundary condition with an optimization mode. *Jounal of Atmospheric and Oceanic Technology*, 14, pp.723-34.

da Rosa, A.V., 2005. *Fundamentals of Renewable Energy Processes*. London: Elsevier Academic Press.

Davies, A.M. & Kwang, S.C., 2000. Tidal Energy Fluxes and Dissipation of The European Continental Shelf. *Journal of Geophisics Research*, 105, pp.21969-89.

Davis Jr., R.A., 1987. *Oceanography: an Inntroduction to The Marine Environment*. Dubuque, Iowa: Wm. C. Brown Publisher.

Egbert, G., Bennett, A. & Foreman, M., 1994. TOPEX/Poseidon tides estimated using a global inverse model. *Journal of Geophysic Research*, 99, pp.24,821 - 24, 852.

Egbert, G.D. & Erofeeva, S.Y., 2002. Efficient inverse modeling of barotropic ocean tides. *Journal of Atmospheric and Oceanic Technology*, 19.

Egbert, G.D. & Erofeeva, L., 2009. *OSU Tidal Data Inversion*. [Online] Available at: http://www.oce.orst.edu/research/po/research/tide/ind.html [Accessed 21 May 2009].

Energy Systems Research Unit's of The University of Strathclyde in Glasgow, 2004. *Marine Current Energy Baseload Supply Strategy for Scotland*. [Online] Available at: http://www.esru.strath.ac.uk/EandE/Web_sites/03-04/marine/index2.htm [Accessed 28 May 2009].

Energy Systems Research Unit's of The University of Strathclyde in Glasgow, 2006. *Marine Current Resource and Technology Methodology*. [Online] Available at: http://www.esru.strath.ac.uk/EandE/Web_sites/05-06/marine_renewables/home/welcome.htm [Accessed 1 June 2009].

Environmental Change Institute, 2005. *Characteristics of the United Kingdom Tidal Current Power Resource*. The Carbon Trust.

EU Commission, 1996. *The exploitation of tidal marine currents*.

Ezer, T., Arango, H. & Shchepetkin, A.F., 2002. Development in terrain-following ocean models: intercomparison of numerical aspects. *Ocean Modelling*, 4, pp.249-67.

Ezer, T. & Mellor, G.L., 2004. A generalized coordinate ocean model and a comparison ofthe bottom boundary layer in terrain-following and in z-level grids. *Ocean Modelling*, 6, pp.379-403.

Faber Maunsell and Metro Plc., 2007. *Scottish Marine Renewable Strategic Environmental Assessment (SEA): Environmental Assessment*. EIA Report. The Scottish Executive.

Flather, R., 1987. Atidal model of the Norteast Pacific. *Atmosphere - Ocean*, 25(1), pp.22-45.

Fraenkel, P., 1999. *Tidal currents: a major new source of energy for the millenium*. London: ICG Publishing Ltd.

Fraenkel, P., 2007. Marine current turbines: pioneering the development of marine kinetic energy converters. In *IMechE Vol. 221 Part A: J. Power and Energy*., 2007.

Frandsen, S. et al., 2006. Analytical Modelling of Wind Speed Deficit Offshore Wind Farms. *Wind Energy*, 9, pp.39-53.

Freris, L. & Infield, D., 2008. *Renewable Energy in Power Systems*. Chichester, West Sussex: John Wiley & Sons Ltd.

Garrett, C. & Cummins, P., 2005. Generating Power from Tidal Currents in Channels. In *R. Soc. Land A*., 2005.

Godin, G., 1972. *The Analysis of Tides*. Toronto: University of Toronto Press.

Griffies, S.M. et al., 2000. Developments in ocean climate modelling. *Ocean Modelling*, 2, pp.123-92.

Gross, M.G. & Gross, E., 1996. *Oceanoggraphy: A View of Earth*. 7th ed. New Jersey: Prentice-Hall.

Hermawan & Hadi, S.P., 2006. Existing Sustainable (Renewable) Energy System in Indonesia. In *The 2nd Joint International Conference on Sustainable Energy and Environment*. Bangkok, 2006.

Hydro-Oceanographic Servive Indonesian Navy, 2009. *Tidal Stream Tables*. Jakarta: Hydro-Oceanographic Servive Indonesian Navy.

Hydro-Oceanographic Servive Indonesian Navy, 2009. *Tide Tables of Indonesian Archipelago*. Jakarta: Hydro-Oceanographic Servive Indonesian Navy.

Indonesia's Centre for Data and Information on Energy and Mineral Resources , 2008. *Indonesia Energy Statistics 2008*. Jakarta: Ministry of Energy and Mineral Resources.

Indonesia's Centre for Data and Information on Energy and Mineral Resources, 2006. *Blueprint of Indonesia's Energy Management 2006 - 2010*. Jakarta: Ministry of Energy and Mineral Resources.

Indonesia's Centre for Data and Information on Energy and Mineral Resources, 2008. *Key indicator of Indonesia energy and mineral resources*. Jakarta: The Ministry of Energy and Mineral Resources.

Intergovernmental Panel on Climate Change, 2007. *Climate Change 2007: Synthesis Report*. Assessment Report. Valencia: Intergovermental Panel on Climate Change.

Kaltschmitt, M., Streicher, W. & Wiese, A., 2007. *Renewable Energy: Technology, Economics, and Environment*. New York: Springer.

Klymak, J.M. et al., 2006. An estimate of energy lost to turbulence at the Hawaiian Ridge. *Journal of Physical Oceanography*, 36(6), pp.1148-64.

Kobold Nusa, 2008. *Tidal Stream Survey in Pringgabaya, East Lombok*. Bandung.

Koropitan, A.F. & Ikeda, M., 2008. Three-dimensioanal modelling of tidal circulation and mixing over the Java Sea. *Journal of Oceanography*, 64, pp.61-80.

Lee, C. et al., 2006. Internal tides and turbulence along the 3000-m isobath of the Hawaian Ridge with model comparison. *Journal of Physical Oceanography*, 26(6), pp.1165-83.

MacKay, D., 2008. *Under-estimation of the UK Tidal Resources*. Cavendish Laboratory, University of Cambridge.

Mellor, G.L., 2004. *User Guide for A Three-dimensional, Primitive Equation, Numerical Ocean Model*. Princeton: Princeton University.

Mellor, G. & Yamada, T., 1985. Development of a turbulence closure model for geophysical fluid problems. *Journal of Geophysics Research*, 90, pp.903-16.

Millar, D.L., 2007. Wave and Tidal Power. In F. Armstrong & K. Blundell, eds. *Energy. Beyond Oil.* Oxford: Oxford University Press. pp.50-70.

Myers, L.E., 2006. *Operational Parameters of Horizontal Axis Marine Current Turbines*. PhD Thesis. Southampton: University of Southampton.

Myers, L. & Bahaj, A., 2005. Simulated Electrical Power Potential Harnessed by Marine Current Turbine Arrays in the Alderney Race. *Renewable Energy* , 30, pp.1713-31.

Oey, L.-Y., 2006. An OGCM with movable land-sea boundaries. *Ocean Modelling*, 13, pp.176-95.

Oey, L.-Y., 2008. *Geophysical fluid experiment with the Princeton Oceanic Model*. Princeton: Princeton University.

Oey, L.-Y., Ezer, T., Hu, C. & Muller-Krager, F.E., 2007. Baroclinic tidal flows and inundation processes in Cook Inlet, Alaska: numerical modelling and satellite observations. *Ocean Dynamics*, 57, pp.205-21.

Pandey, V.K. & Pandey, A.C., 2007. Turbulent Kinetic Energy and Its Dissipation Rate of the Indonesian Throughflow Region via Lombok and Savu Straits. *Journal of India Geophysic Union*, 11(2), pp.117-22.

Pangastuti, W., 2005. *Study of tidal use in Seribu Islands Area*. Bsc Final Project. Bandung: Bandung Institute of Technology.

Powlowicz, R., Beardsley, B. & Lentz, S., 2002. Classical Tidal Harmonic Analysis Including Error Estimates in MATLAB using T_TIDE. *Computer Geosience*, 28, pp.929-37.

Reeve, D., Chadwick, A. & Fleming, C., 2004. *Coastal Engineering: Process, Theory and Design Practice*. Oxon: Spon Press.

Russell, R.C.H. & Macmillan, D.H., 1954. *Waves and Tides*. 2nd ed. London: Hutchinson's Scientific and Technical Publications.

Schiller, A., 2004. Effects of explicit tidal forcing in an OGCM on the water-mass structure and circulation in the Indonesian throughflow region. *Ocean Modelling*, 6, pp.31-49.

Short, J.C.A., 2007. *A Hydrodynamic Modelling Investigation into Tidal Asymmetry and Its Impact on Sedimennt Transport; Southampton Water, UK*. Southampton: University of Southampton.

Shulman, I. & Lewis, J.K., 1995. Optimization approach to the treatment of open boundary condition. *Journal of Physical Oceanography*, 25, pp.1006-11.

Smith, W.H.F. & Sandwell, D.T., 1997. *Global Seafloor Topography from Satellite Altimetry and Ship Depth Soundings*. Science.

Sorensen, R.M., 2006. *Basic Coastal Engineering*. Third Edition ed. New York: Springer.

Speetjens, F. & Pittenger, J., 2008-2009. *Tidal Power: The Renewable Energy Source of Tacoma's Future*. [Online] Available at: http://tidaltacoma.com/Gorlov_Turbine.html [Accessed 1 June 2009].

Thake, J., 2005. *Development, Installation, and Testing of A Large Scale Tidal Current Turbine*. Technical Report. Departement of Trade and Industry, UK.

The Carbon Trust, 2009. *Technical overview of wave and tidal stream energy*. [Online] Available at: http://www.carbontrust.co.uk/technology/technologyaccelerator/ME_guide.htm [Accessed 26 May 2009].

The Carbon Trust, 2009. *Tidal streams and tidal stream energy device design*. [Online] Available at:

http://www.carbontrust.co.uk/technology/technologyaccelerator/ME_guide3.htm [Accessed 26 May 2009].

Thurman, H.V., 1997. *Introductory Oceanography*. 8th ed. New Jersey: Prentice-Hall.

Twidell, J. & Weir, T., 2006. *Renewable Energy Resources*. 2nd ed. Oxon: Taylor & Francis.

WS Atkins Consultants and members of the NSC, 2006. *Best Practice Guidelines for Marine Applications of Computational Fluid Dynamics*. MARNET CFD.

Zhang, A., Wei, E. & Parker, B.B., 2003. Optimal estimation of tidal open boundary conditions using predicted tides and adjoint data assimilation techniques. *Continental Shelf Research*, 23, pp.1055-70.

LIST OF APPENDICES (SEE ATTACHED CD)